Biogeochemistry (2007) 85:263–288
DOI 10.1007/s10533-007-9133-z

ORIGINAL PAPER

Dissolved reactive phosphorus in large rivers of East Asia

Lingling Wu · Youngsook Huh

Received: 28 February 2006 / Accepted: 15 May 2007 / Published online: 27 July 2007

Abstract Dissolved reactive phosphorus (DRP) concentrations in large pristine rivers of East Asia (370 samples) are reported and the relationship to lithology (phosphorites, igneous apatite-bearing deposits), relief, climate (precipitation, temperature), and population density are investigated. The DRP concentration and yield of 93% of our samples were distinctly low (<0.06–0.89 μM DRP and <0.0008–800 mol DRP/km^2/year). The samples with relatively high DRP (~7% of our samples) were most likely from point sources of human sewage rather than P-rich lithology. The principal component analyses using DRP, dissolved major elements, pH, Sr, and $^{87}Sr/^{86}Sr$ found DRP best grouped with dissolved Si and K. However, the correlation between DRP and dissolved Si is still not strong enough to justify using Si as a proxy of DRP export by chemical weathering. The large rivers draining the eastern Tibetan Plateau—the headwaters of the Mekong, Yangtze, and Yellow—together supplied 3.0×10^7 mol DRP/year, 7%, 3%, and 17% of those at mouths, respectively, and were not dominant source regions of DRP. The mouth values of the East Siberian rivers were especially low and this was due to multiple factors, e.g., low precipitation and sparse population. Stepwise regression of various parameters like precipitation, temperature, runoff, population density and relief indicated that the concentrations were not affected by any single factor, but precipitation and secondarily population density explained up to 44% of the variability in the DRP yield of the East Asian rivers.

Keywords Dissolved reactive phosphorus · Factor analysis · Nutrient · Siberia · Tibet · Weathering

L. Wu · Y. Huh
Department of Earth and Planetary Sciences, Northwestern University, 1850 Campus Drive, Evanston, IL 60208-2150, USA

Y. Huh (✉)
School of Earth and Environmental Sciences and Research Institute of Oceanography, Seoul National University, San 56-1, Sillim 9-dong, Gwanak-gu, Seoul 151-747, Korea
e-mail: yhuh@snu.ac.kr

Introduction

Phosphorus (P) is an essential and often limiting nutrient which can regulate the rate of biological productivity in terrestrial and aquatic ecosystems. Primary productivity in turn determines how fast atmospheric CO_2 is assimilated into organic matter, and thus the P cycle is closely coupled to the carbon cycle and global climate change. On geologic time scales (>1 My), the most important pre-industrial supply of P to the oceans is riverine transfer from continental weathering of P-bearing igneous and sedimentary rocks (Meybeck 1993; Filippelli and Delaney 1994; Delaney 1998; Guidry and Mackenzie

2000). The eolian P flux to the surface oceans is less than 10% of the riverine input (Froelich et al. 1982; Compton et al. 2000). In the oceans, P is removed by sequestration in marine sediments (authigenic carbonate fluorapatite, biogenic apatite, organic matter, iron–manganese oxides, and carbonates) (Froelich et al. 1982; Meybeck 1993; Compton et al. 2000; Schenau et al. 2005). Models of the global P cycle have assumed that P flux from continental weathering will increase with enhanced weathering rates (Colman et al. 1997; Compton et al. 2000; Guidry et al. 2000). If P flux from continents to the oceans is controlled by weathering of disseminated apatite (Ruttenberg and Berner 1993; Filippelli 1997), riverine P flux will scale with global average chemical weathering rates. On the other hand, if weathering of phosphorites, i.e., sedimentary rocks with >15 wt% P_2O_5 (Boggs 2001), is important, the exposure and weathering rates of phosphorites specifically will be the controlling factor. Related to the issue of lithology is what controls the weathering rate of the relevant continental P-reservoir. In this study, we addressed the effect of lithology and factors that control the weathering rates of the relevant continental P reservoirs, e.g., physiography (relief) and climate (precipitation, temperature).

Phosphorus is present in most rocks in trace amounts, averaging 0.12 wt% P_2O_5 in continental sediments (Li 2000) and 0.15% in the upper continental crust (UCC) (Rudnick and Gao 2004). In igneous rocks, it takes the form of apatite, with values commonly between 0.01% and 0.5% P_2O_5 and as high as 1.5–2.0% P_2O_5 in strongly alkaline, low-silica igneous rocks (Nash 1984). Apatite is also a common accessory mineral in metamorphic rocks, yet the details of its occurrence are not well known (Nash 1984).

Dissolved reactive phosphorus (DRP), also referred to as soluble reactive phosphorus (SRP), is operationally defined as the colorimetrically detected orthophosphate (PO_4^{3-}, HPO_4^{2-}, $H_2PO_4^-$) and various ion-pairs with contributions from organophosphorus compounds and inorganic polyphosphates that are hydrolyzed to reactive phosphate during the analytical procedure (House et al. 1995). In rivers, although around 95% of P occurs in particulate form (Meybeck 1982), DRP is the most readily bioavailable form and thus directly coupled with phytoplankton blooms in coastal regions or lakes and organic matter burial in oceans, which in turn will govern the authigenic carbonate fluorapatite deposition (Ruttenberg 2004). Although small organic molecules can sometimes be assimilated (Cotner and Wetzel 1992), most organic P must be released from the organic moiety through hydrolytic action by enzymes before it is available for assimilation (Ekholm 1994; Shan et al. 1994; Seitzinger et al. 2005).

The global riverine flux of dissolved P has been estimated and modeled by a number of workers (Froelich et al. 1982; Meybeck 1982, 1993; Smith et al. 2003; Turner et al. 2003; Harrison et al. 2005), and the global average DRP concentration has been estimated as 0.32 μM (Meybeck 1982) and the global annual riverine flux as (1.3–8.4) × 10^{10} mol/year (Meybeck 1982; Turner et al. 2003). However, these compilations lacked DRP data for the large pristine rivers such as Salween, Red, Omoloy and Anadyr in East Asia or the headwaters of major rivers like the Yellow, Yangtze, and Mekong. Previous studies on nutrients of Asian rivers were on lower reaches (Cauwet and Sidorov 1996; Lara et al. 1998; Holmes et al. 2000, 2001; Liu et al. 2003) or estuaries (Edmond et al. 1985; Zhang 1996) focusing on direct anthropogenic impact and eutrophication. They reported very low concentrations of DRP (0.2–1 μM) in the Lena River in Eastern Siberia and elevated nutrient levels in Chinese rivers (0.57 μM DRP for the Yangtze, and 0.36 μM DRP for the Yellow), the latter probably due to extensive use of chemical fertilizers as well as domestic sewage input in the middle and lower reaches. We obtained new DRP data on the headwaters of the East Asian rivers and examined the controlling factors on riverine DRP concentrations and fluxes in areas not significantly affected by anthropogenic inputs.

We aimed to (1) enlarge the database for natural systems to aid in global P modeling and (2) understand natural and human controls on the delivery of P to surface fresh waters.

Study area

Location and geologic setting

The East Asian rivers considered here originate in the elevated continental interior and flow ultimately into the Indian, Pacific and Arctic oceans (Fig. 1). The

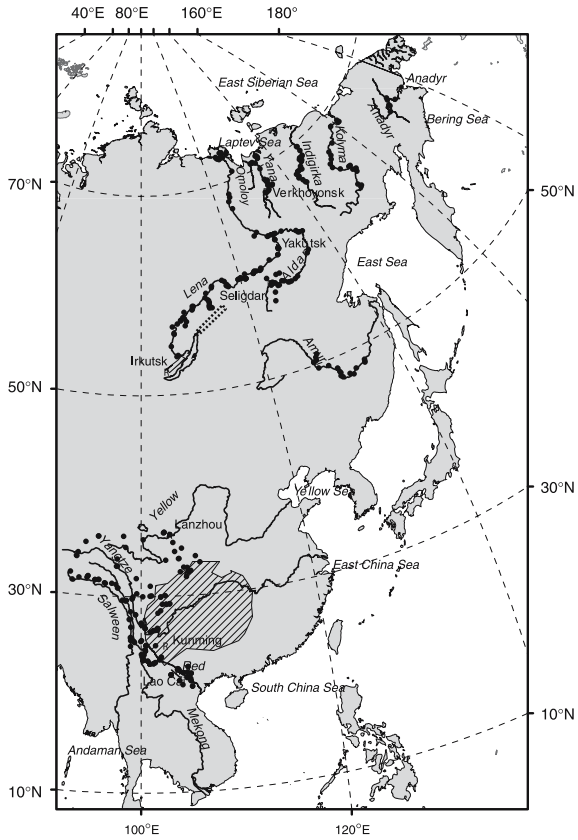

Fig. 1 The location map of the major rivers of East Asia. The cross-hatched area in China is the Late Proterozoic-Early Cambrian phosphorite deposits of the Yangtze Platform (modified from Li 1986). Dotted area northeast of Lake Baikal marks the igneous apatite-bearing deposits in Siberia (Notholt 1980), and the dotted area west of Lake Baikal is the phosphorite bed. The black dots indicate our sampling sites

Salween, Mekong, Red (Hong He), Yangtze (Chang Jiang), and Yellow (Huang He) rivers drain the eastern Tibetan Plateau region and the Amur, Lena, Omoloy, Yana, Indigirka, Kolyma and Anadyr drain the vast Russian Far East. The eastern Tibetan Plateau is a region where several terrains have come together in the Devonian to Late Triassic associated with the closing of the paleo-Tethys. The Red River flows along the NW–SE trending Red River Fault Zone in South China and North Vietnam, formed after collision of Eurasia and India in the Cenozoic. The Lena drains the sedimentary platform and basement terrain of the Siberian Craton. The basement is exposed in the Aldan Shield and Trans-Baikal Highlands south of the Craton and drained by the upper right bank tributaries of the Lena and the Upper Amur. To the east, the Lower Lena and Omoloy, Yana, Indigirka, Kolyma and Anadyr drain a Mesozoic continental collisional/accretionary zone of complex lithology (Huh et al. 1998a, b; Huh and Edmond 1999; Zakharova et al. 2005).

An overview of the major rock types in our drainage basins is provided by the global surficial lithology map (Dürr et al. 2005). In the Upper Salween and Mekong drainage basins, siliciclastic (Ss: <10% carbonate), mixed (Sm: ~40% carbonate), and carbonate (Sc: ~80% carbonate) consolidated sedimentary rocks occur with some metamorphic rocks (Mt). In the Upper Red and Yangtze basins, Ss and Sm are most common with some Mt. The Upper Yellow drains through Sm and minor loess and semi- to unconsolidated sedimentary rocks (Su). In the Amur basin, Su, Mt and Quaternary alluvial deposits (Ad) are found, and in the Lena basin, Sc, Ss, Su, Mt and Ad are all found. Other rivers of the Russian Far East (Omoloy, Yana, Indigirka, Kolyma, and Anadyr) drain through Ss, Ad, Mt and some basic volcanic rocks (Vb).

Since disseminated apatite minerals are by definition homogeneously distributed in sedimentary and igneous rocks and affect all samples, we focused on the spatial distribution of phosphorites and igneous apatite. Within our sample drainage basins, there are no world-class phosphorite deposits on the scale of Hubsugul (Mongolia) or Duchess (Australia), Aktyubinsk (Russia) or Kunming (China) (Cook 1984). However, there are some major provinces of Late Proterozoic and Cambrian age, believed to be the greatest global phosphogenic episode in geological history (Notholt et al. 1986). In the Russian Far East, there are thin phosphorite beds along the western shore of Lake Baikal to the upper reaches of the Lena River and in the Trans-Baikal Highlands in northeastern Irkutsk (Fig. 1) (Notholt et al. 1986). In China, phosphorites are widely distributed on the Yangtze Platform in the south (Fig. 1) (Li 1986). In northern Vietnam, metamorphosed phosphorite deposits were found near Lao Cai extending along the southwest of the Red River in a zone 1–4 km wide (Fig. 2c) (Tran and Nguyen 1986). These deposits contain 10–36% P_2O_5, which are the highest grades associated with secondary deposits produced by weathering.

The apatite deposits of igneous origin are less widely distributed than those of sedimentary origin

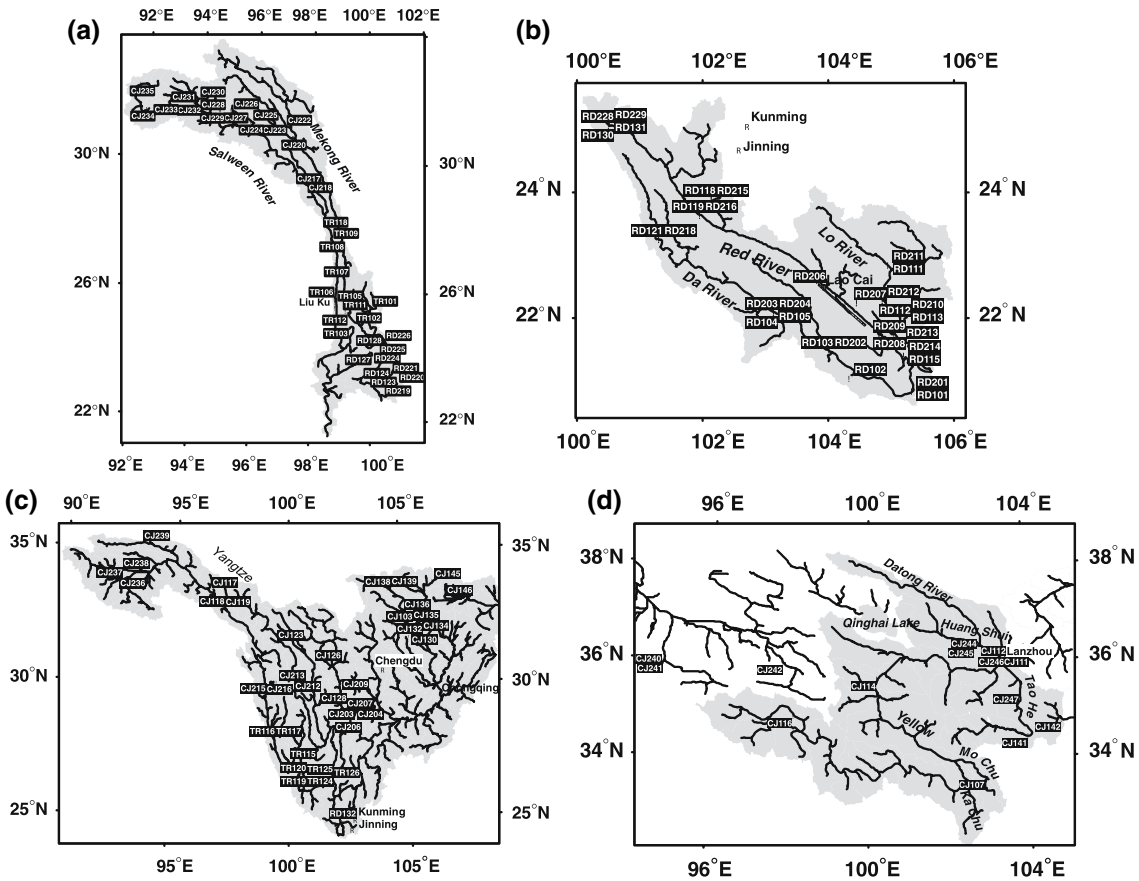

Fig. 2 The sample location maps of the (**a**) Salween and Mekong, (**b**) Red, (**c**) Yangtze, and (**d**) Yellow rivers. The narrow belt along the Red main channel is the Lao Cai phosphorite deposit, modified from Tran et al. (1986). Authors can be contacted for higher resolution map

(Notholt 1980). In our study area, an alkaline complex hosted a narrow (up to 400 km) belt of igneous apatite (at most 4% P_2O_5) extending northeastwards from the northern end of Lake Baikal (Fig. 1, 3b) (Notholt 1980). The Seligdar apatite deposit (7 × 25 km area close to the city Seligdar) (Fig. 1) in the central part of the Precambrian Aldan Shield contains 4–10% P_2O_5 (Ilyin and Krasilnikova 1989).

Climate

The drainage basins in the Russian Far East experience continental climate with cool, wet summers and cold, dry winters (Huh et al. 1998b). Precipitation occurs mostly in summer, and the area is free from glaciers except in the highest alpine elevations. The Yangtze, Yellow, and Amur drainage basins are under the influence of the East Asian subtropical monsoon, and the Salween, Mekong and Red rivers are affected by the Indian monsoon system (Wang et al. 2003). The summer monsoon is stronger in India than in East Asia, whereas the winter monsoon is more intense in East Asia (Wang et al. 2003). As a result, the Salween, Mekong and Red river basins experience higher precipitation and temperature than the Yellow and Amur basins in summer. The annual runoff of the Salween, Mekong, and Red rivers (~420–570 mm/year) is about twice that of the other rivers studied here (Table 1).

Methods

Sampling expeditions were made in July–September over the period of 1991–1997 for the Russian Far East and in May–September of 1998–2004 and in

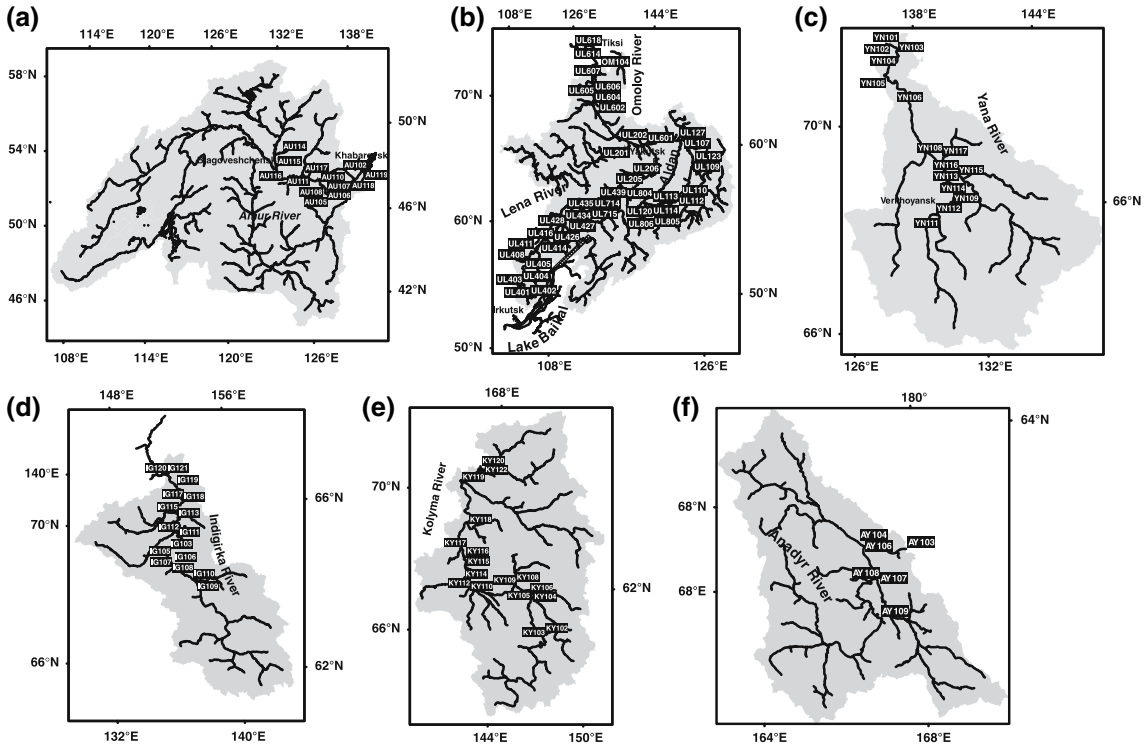

Fig. 3 The sample location maps of the (**a**) Amur, (**b**) Lena and Omoloy, (**c**) Yana, (**d**) Indigirka, (**e**) Kolyma, and (**f**) Anadyr rivers. The narrow shaded area north of Lake Baikal shows the igneous apatite-bearing deposits in Siberia (Notholt 1980). Authors can be contacted for higher resolution map

December–January of 2002–2003 for western China and northern Vietnam (Tables A1–A2). River water samples were filtered through 0.45 μm cellulose acetate membrane filters in the field and stored in pre-cleaned glass containers. The filtrate was acidified to pH ~2 with pure HCl or HNO_3. DRP concentrations were determined by direct colorimetric method (APHA 1998), in which ammonium molybdate and potassium antimony tartrate reacted with orthophosphate to form a heteropoly acid and then reduced to intensely colored molybdenum blue by ascorbic acid. Our detection limit was 0.06 μM phosphate using 100 mm cuvette. The detection limit was 0.03 μM if calculated by three times the standard deviation of the blank concentration. But considering the large relative error (absolute error divided by the average concentration for replicate analyses) (up to 0.75) when concentrations were below 0.06 μM, we chose 0.06 μM as our detection limit. The relative error was within 10% when concentration was above 0.06 μM. Diluted tap water which is kept at room temperature and used as a reference has a 4.6% relative standard deviation.

The bed sediment samples were collected from the top 5–10 cm of the river bed. The samples were air-dried and the < 500 μm size fraction was separated by sieving to remove the gravel and plant debris. For sample number TR100 series (Table A1; sampled in August 2004 for Salween, Mekong and Yangtze), additional separation was made between the sand (63–500 μm) and silt (2–63 μm) size fractions, and the weighted bulk % P_2O_5 was calculated. Phosphorus content was measured using ARL3560 ICP-ES after $LiBO_2$ fusion at XRAL laboratories in Ontario, Canada. The detection limit was 0.01 wt% P_2O_5 and the precision was within ±0.01 wt% for 16 different duplicates. Only one duplicate (CJ137) had 0.09 wt% difference.

Factor analysis was applied to explain the variance in the observed chemical compositions (DRP, major elements, pH, Sr, and $^{87}Sr/^{86}Sr$). We used Na normalized ratios in order to eliminate the dilution

Table 1 Dissolved reactive phosphorus (DRP) fluxes of the large rivers of East Asia

River name	Sample number	Drainage area[a] 10^3 km^2	Runoff[a] mm/year	Relief[a] m	Population density[a] indiv./km^2	Total P in Soil[b] 10^3 mol/km^2	DRP concentration		DRP flux	DRP yield	
							This study μM	Literature[c] μM	This study 10^6 mol/year	This study mol/km^2/year	Literature[c] mol/km^2/year
Salween[d]	*TR103*	*108*	*534*	*857*	*7.52*	*3,225*	*0.54*	–	*31*	*288*	–
Mekong	*RD126/RD223*	*127*	*421*	*1,245*	*21.5*	*3,230*	*0.21*	*0.27*	*11*	*88*	*192*
Red[e]	RD101/RD201 RD115/RD214 RD114/RD213	136	566	985	66.6	1,716	0.41	–	31	231	–
Yangtze	*TR126*	*238*	*294*	*3,645*	*11.8*	*3,043*	*0.18*	*0.35*	*12*	*52*	*216*
Yellow	*CJ246*	*232*	*172*	*794*	*24.5*	*2,735*	*0.17*	*0.65*	*6.9*	*30*	*54*
Amur	AU102	1,604	143	653	22.3	2,674	0.42	0.68	97	61	288
Lena	UL607	2,372	181	697	0.24	2,809	0.09	0.21	39	16	46
Omoloy	OM104	32	25	573	0.03	3,168	<0.06	–	<0.05	<1	–
Yana	YN101	228	88	809	0.04	3168	0.16	0.36	3.1	14	52
Indigirka	IG121	303	133	898	0.02	3,168	0.11	0.22	4.5	15	37
Kolyma	KY120	645	156	669	0.02	3,095	<0.06	0.35	<6.0	<9	47
Anadyr	AY103	158	287	554	0.0004	3,086	<0.06	–	<2.7	<17	–
Average		515	250	1032	13	2,926	0.25	0.39	26	88	117

[a] Drainage area data from Hearn et al. (2000, 2001), runoff from Fekete et al. (2002), relief from the NGDC digital topographic database, and population density from Hearn et al. (2003)

[b] Total P was calculated for top 20 cm of soils: area percentage of soil orders in the drainage basin x concentration of total P in each soil order (Okin et al. 2004)

[c] Literature values from Global Environmental Monitoring Systems (1994–1996), Meybeck and Ragu (1996), Holmes et al. (2000), Yan and Zhang (2003), Harrison et al. (2005)

[d] Rows in italics indicate rivers which are sampled in the upper reaches while others have been sampled at the mouth

[e] The DRP concentration is a discharge-weighted average and the DRP yield, relief, and population density are area-weighted averages using the furthest downstream samples of the three tributaries that made up the Red River-the Da, Red main channel, and Lo

effect with higher runoff (Gaillardet et al. 1999). The principal components analysis (PCA) of SPSS v. 12.0 was used, and in order to avoid singularity and multicollinearity problems we screened the data prior to the main PCA and eliminated the HCO_3/Na ratio (very high correlation coefficients of 0.928 with Mg/Na and 0.958 with Ca/Na). The Kaiser–Meyer–Olkin measure of sampling adequacy was 0.649 (>0.5), indicating that factor analysis was appropriate for these data (Kaiser and Rice 1974; Hutcheson and Sofroniou 1999). Although the concentrations for the DRP and major ions do not follow normal distributions, the repeatability of principal components in the samples was not severely affected (Dudzinski et al. 1975). Varimax rotation was used to improve the interpretability of factors.

A stepwise multiple regression using DRP yield, river water temperature, monthly precipitation, monthly evapotranspiration, and monthly runoff was performed on the 54 summer–winter samples to investigate the correlations between DRP yield and the climatic parameters. The same approach was also applied to the full dataset (all from high water stage) to examine the correlations between DRP yield and annual precipitation, annual runoff, population density and relief. The criteria were $F \leq 0.05$ for entry and $F \geq 0.10$ for removal.

We used ArcGIS® software to calculate the drainage basin area, precipitation, evapotranspiration, runoff, relief, and population density for each of our sample basins. The drainage basin area, precipitation, and evapotranspiration data were modified from the USGS Global GIS database for South Asia (Hearn et al. 2000) and North Eurasia (Hearn et al. 2001) which in turn were based on the 30 arc-second digital elevation model (DEM) of the world (GTOPO30). Runoff data were from the UNEP/GRDC Composite Runoff Fields v 1.0, interpolated from values measured at hydrological stations (Fekete et al. 2002). The mean local relief, defined as the mean of ''maximum–minimum'' elevation within each 10-min grid (Summerfield and Hulton 1994) was calculated from the 10-min gridded elevation data from the National Geophysical Data Center digital topographic database (http://www.ngdc.noaa.gov/mgg/global/relief/ETOPO5/TOPO). The population density data were from the DVD version of USGS Global GIS dataset (Hearn et al. 2003) and the original data were from Landscan Global Population 2000 Database compiled on $30'' \times 30''$ grids created by Oak Ridge National Laboratory (Dobson 2000). To calculate the areal percentage of soil orders in the drainage basins, we used an order-level global soil map rasterized on 2-min grid cells available from the USDA National Resource Conservation Service. This was based on the global soil map produced by the UNESCO FAO and digitized by ESRI (http://www.soils.usda.gov/use/worldsoils/mapindex/order.html).

We computed the hydroxyapatite saturation index (HSI) using the Geochemist's Workbench v.4.0 (Bethke 2002) and the thermodynamic database provided with the program. HSI is defined as $\log(\{Ca^{2+}\}^5\{PO_4^{3-}\}^3\{OH^-\}/K_{hydroxyapatite})$ where {} denotes activity.

Results and discussions

Concentrations and yields of dissolved reactive phosphorus

The measured concentrations of DRP and P_2O_5 contents of bed sediments are listed in Tables A1 and A2. The total range in DRP was from <0.06 to 4 μM, but median values were relatively homogeneous (<0.06–0.49 μM) regardless of drainage basin (Fig. 4). In comparison, the global average was estimated to be 0.32 μM using the 1970s data of pristine rivers (Meybeck 1993) or 0.56 μM using 1990s data (Smith et al. 2003). The median DRP values were generally very low in the East Siberian rivers with the exception of the Amur and the Yana (Fig. 4). The median DRP yields ranged from <4 to 207 mol/km^2/year for high water stage samples and were also low in East Siberian rivers (Fig. 5). No correlation existed between DRP/Na and Mg/Na, Cl/Na, SO_4/Na, Sr/Na, pH and $^{87}Sr/^{86}Sr$ at a 5% significance level. Experimental studies have suggested that low pH and high sulfate in water tended to promote the mobility of P in soils (Koerselman et al. 1993), but such an effect was not discernible at the scale of river drainage basins in East Asia.

For each major river basin, we compiled data for the furthest downstream locations sampled in order to (1) quantify the contribution of headwaters to the DRP of the entire basin in the case of the Salween, Mekong, Yangtze and Yellow rivers and (2) to compare the mouth values obtained in our study with

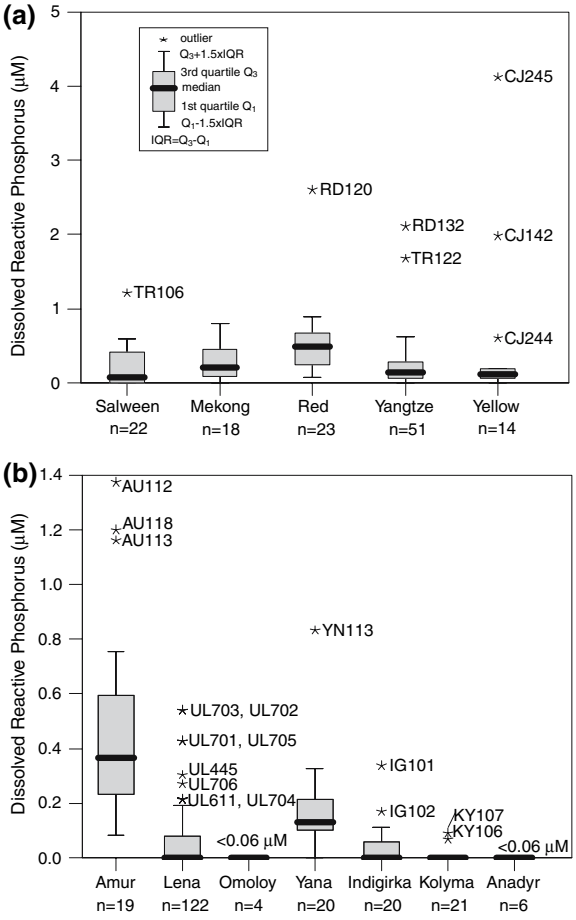

Fig. 4 Box plots of DRP concentration in (**a**) the Vietnamese and Chinese rivers (Salween, Mekong, Red, Yangtze, and Yellow) and (**b**) the Russian rivers (Amur, Lena, Omoloy, Yana, Indigirka, Kolyma, and Anadyr). Notice the difference in y-scale between (**a**) and (**b**). The number of samples analyzed for each basin is indicated by *n*. Stars are outliers (7% of the total number of samples) and are labeled with the sample I.D. All samples included in the plots are from high water stage

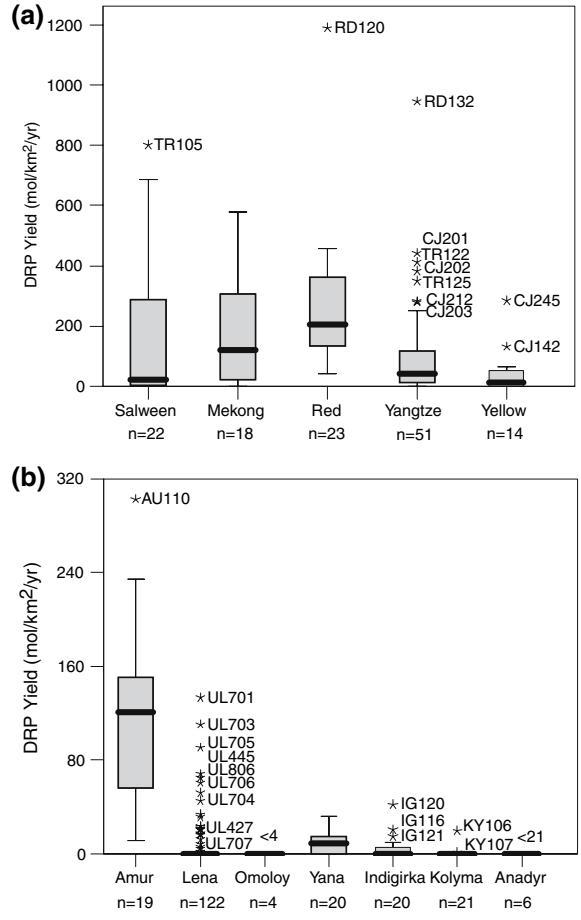

Fig. 5 Box plots of DRP yields of (**a**) the Vietnamese and Chinese rivers and (**b**) the Russian rivers. Notice the difference in y-scale between (**a**) and (**b**). The number of samples analyzed for each basin is indicated by *n*. Stars are outliers and are labeled with the sample I.D. All samples included in the plots are from high water stage

literature values in the case of the Red, Amur, Lena, Omoloy, Yana, Indigirka, Kolyma, and Anadyr (Table 1). We were not able to find literature DRP values for the mouths of Salween, Red, Omoloy and Anadyr rivers.

During the rising water stage of summer, the DRP concentrations of the Upper Mekong, Yangtze and Yellow were 78%, 51%, and 26% of the mouth values, respectively, and the DRP fluxes were 7%, 3%, and 17% of the delivery at mouths, respectively (Table 1). The low nutrient levels in the upper reaches of the Yangtze were in agreement with a previous study focusing on the spring season (Liu et al. 2003). On the tributary scale, the concentration values we report for Dadu He and Yalong Jiang (0.62 vs. 0.062 μM and 0.15 vs. 0.12 μM) were higher than those reported by Liu et al. (2003) but lower than those reported for Jialing Jiang and Fou Jiang (0.31 vs. 0.99 μM and <0.06 vs. 0.8 μM). The same held for DRP yields for these tributaries. The DRP yields in the upper Mekong, Yangtze, and Yellow rivers were 46%, 24%, and 56% of the entire basin, suggesting that significantly greater amount of P per unit area came from the lower reaches. The rivers originating in the eastern Tibetan Plateau (Salween, Mekong, Yangtze, and Yellow) together supplied 6.1×10^7 mol DRP/

Table 2 Rotated component matrix[a] showing loadings for each dissolved major element onto each factor and total variance explained by the principal component analysis

	Factor			
	1	2	3	4
Ca/Na	0.82	0.40	–	–
Mg/Na	0.79	–	–	–
Sr/Na	0.77	–	–	–
SO_4/Na	0.76	–	–	–
DRP/Na	–	0.83	–	–
Si/Na	–	0.76	−0.47	–
K/Na	–	0.70	–	–
Cl/Na	–	–	0.76	–
pH	–	–	0.73	–
$^{87}Sr/^{86}Sr$	–	–	–	0.88
% Of variance explained	27	21	15	11
Cumulative %	27	48	63	74

[a] Rotation method: varimax with Kaiser normalization

–, Loading smaller than 0.4 and thus considered not important (Field 2000)

year, 9% of the mouth value (assuming same concentration for the mouth of Salween as our headwater). The eastern Tibetan Plateau region was not a major source of DRP yield even though it generated significant amounts of dissolved major elements and suspended material (e.g., Wu et al. 2005; Qin et al. 2006). Our DRP concentration of the Amur at mouth was about 40% lower than that reported in Meybeck and Ragu (1996) and the yield was ~20% of the literature value. Also, the DRP at the mouths of the Arctic rivers (Lena, Yana, Indigirka and Kolyma) in this study (summer samples in multiple years) were always lower than those of Holmes et al. (2000) averaged for 12 months (Table 1).

Controls on riverine DRP

We applied factor analyses to the DRP and dissolved chemical data (see ''Methods'' section) to derive source characteristics of the DRP. Four factors have been extracted from the principal components analysis, accounting for 74% of the variance in the data set (Table 2). The first factor had high positive loadings (>0.7) for Ca/Na, Mg/Na, Sr/Na, and SO_4/Na ratios and could be interpreted as weathering of carbonates and associated gypsum. The second factor had high positive loadings (>0.7) for DRP/Na, Si/Na, and K/Na. The Si/Na, K/Na, and Ca/Na were positively correlated with DRP/Na and the correlations were significant at a 5% level although the correlation coefficients were low (R^2 = 0.22, 0.17, and 0.012, respectively). As DRP, Si, and K are all important nutrients, the second factor could be related to biological activities such as uptake in soils and/or streams. Alternatively, weathering of sedimentary silicates with disseminated apatite could also yield such combination of elements. The Cl/Na ratio and pH had high positive loadings (>0.7) on the third factor with a significant negative loading on Si/Na ratio, perhaps indicating halite dissolution or seasalt input relative to silicate weathering. The fourth factor had a single high positive loading (>0.8) on $^{87}Sr/^{86}Sr$.

Effect of lithology

To constrain how lithology affects DRP delivery by rivers, we examined the relationship between DRP and (1) locations of known phosphorite and igneous apatite deposits, (2) P_2O_5 in bed sediments, (3) soil total P content.

Assuming the disseminated apatite to be widespread in sedimentary, metamorphic and igneous rocks and therefore affecting different samples to

similar degrees, we focused on phosphorites and igneous apatite deposits which had more localized exposure. For lack of information on the exact exposure within our drainage basins, we were limited to only qualitative comparisons. Samples collected in the vicinity of the phosphorite and igneous apatite deposit locations mentioned in the Geologic Settings section—e.g., Lake Baikal, Aldan Shield, Yangtze Platform, and Lao Cai—did not have noticeably high DRP concentrations or yields except those of the Yangtze Platform. For example, the headwaters of the Lena (UL401–UL403) draining the thin phosphorite beds along the western shore of Lake Baikal (Notholt et al. 1986) contained 0.06 μM (median) DRP, which was only slightly higher than the median value for all Lena samples (<0.06 μM). The Vitim (UL422–UL428), a tributary of the Lena near the apatite-bearing deposits of the alkaline complex (Notholt 1980), also had low DRP concentrations. The Aldan, a tributary of the Lena draining apatite deposits in the central Aldan Shield (Ilyin and Krasilnikova 1989), likewise had median DRP < 0.06 μM. Both summer and winter samples draining the Lao Cai phosphorite deposit (RD106/RD205, RD109/RD208, and RD115/RD214) while higher than the Siberian samples, had similar DRP as the average Red (43 samples) (median 0.48 vs. 0.49 μM). The median DRP yield was also comparable (173 vs. 169 mol/km^2/year). Only the Yangtze Platform samples (n = 21) showed higher median DRP concentrations and yields than the average Yangtze (n = 51, only summer samples) (0.31 vs. 0.16 μM, 117 vs. 41 mol/km^2/year), but they were still lower than the Red River. The absence of correlation, albeit qualitatively, with phosphorites was consistent with model calculation by Guidry et al. (2000) which showed phosphorite to be only a minor reservoir of P in sedimentary rocks, orders of magnitude smaller than continental sediments.

Next, we considered the P_2O_5 content in the bed sediments as representing modified source rock composition after weathering. The P_2O_5 contents of bed sediments for high water stage samples ranged from 0.01 to 0.21 wt% with similar median P_2O_5 (0.09 ± 0.02 wt%) in different rivers (Tables A1–A2, Fig. 6). In the case of the TR100 series samples for the Salween, Mekong and Yangtze, where we had data for different size fractions, the P_2O_5 wt% was around twice as high in the silt size fractions as in the sand size fractions, probably due to dilution with

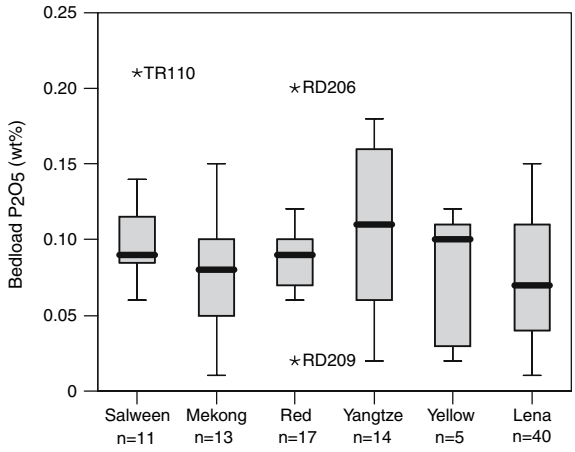

Fig. 6 Box plots of P_2O_5 (wt%) contents in bed sediments of the Salween, Mekong, Red, Yangtze, Yellow and Lena rivers. The number of bed sediment samples for each basin is indicated by n. Stars are outliers (3% of the total number of samples) and are labeled with the sample I.D. Both high and low water stage samples are included

P-poor quartz in the sand size fraction. The P content in bed sediments were mostly lower than the upper continental crust (UCC, 0.15%) (Rudnick and Gao 2004) (Tables A1–A2, Fig. 6). When we normalized for chemical alteration using the immobile element Nb, the P_2O_5/Nb molar ratios likewise were lower than the UCC (82 ± 13) (Rudnick and Gao 2004) for about two thirds of the samples, especially for the Salween, Mekong and Red samples, suggesting loss of P to the dissolved phase during weathering. There was no direct relationship between the DRP and the P_2O_5 content of the bed sediments. We normalized the DRP using Na to account for the variation in discharge and still no relationship was found between the two normalized ratios, DRP/Na and P_2O_5/Nb.

Soil leaching can be regarded as an indirect effect of lithology. We used the global soil map and the P concentrations in the top 20 cm by soil order (Okin et al. 2004) to estimate the total P available to soil leaching. Admittedly this was a crude estimation because of the great heterogeneity of soil P pool between and within orders (Okin et al. 2004; Zhang et al. 2005). Ninety-eight percent of the Red River drainage basin is covered by Ultisols which are soils relatively depleted in P (1.66×10^6 mol P/km^2 in the top 20 cm) having lost the HCl-extractable fraction of P (largely Ca-bound phosphate minerals) by chemical

weathering (Cross and Schlesinger 1995). This suggested that the Red River basin may have been a more significant reservoir of P in the past. Fifty-three percent of the Mekong and 85% of the Salween drainage basins and those of many East Siberian rivers are covered by Gelisols. In coastal continental Antarctica Gelisols have high P content (3.17×10^6 mol P/km^2 in the top 20 cm) due to inputs from seabirds and eolian influx (Beyer et al. 2000), but little is known about P in Gelisols of alpine regions. Inceptisols cover 36% of the Upper Yangtze basin, 50% of Upper Yellow, 51% of the Amur, and 72% of the Lena. These soils are estimated to have moderate P content (2.71×10^6 mol P/km^2 in the top 20 cm) with ~20% of total P HCl-extractable (Cross and Schlesinger 1995). Alfisols have high fertility and are found only in a small area (7%) of the Amur basin. Overall, there was no meaningful relationship between DRP yield and estimated total soil P (Table 1). From the above consideration, there is no evidence for direct lithologic control on DRP in the rivers of East Asia.

Effect of physiography

The mean local relief of the basin had no direct correlation with DRP. The DRP yield in basins with high relief (1–6 km), e.g., the Upper Salween, Mekong and Yangtze, spanned a larger range from <0.1 to 1,000 mol/km^2/year, whereas in basins with lower relief (<1 km) such as the Amur and the East Siberian rivers, the DRP yield had a smaller range from <0.0008 to ~300 mol/km^2/year. If relief were important in controlling physical weathering rates and in turn chemical weathering rates and DRP yields, we might expect high DRP yields in high relief basins. However, we did not see this, perhaps because of the dominance of other potential controlling factors such as climate or population density.

Effect of climate

Climate can affect weathering rates through increase in reaction temperature or through increased hydrologic activity. The temperature-dependence of weathering rates of phosphate minerals was supported by experimental studies. Apatite dissolution and soil incubation experiments have shown that higher temperatures improve the mobilization of P by lowering

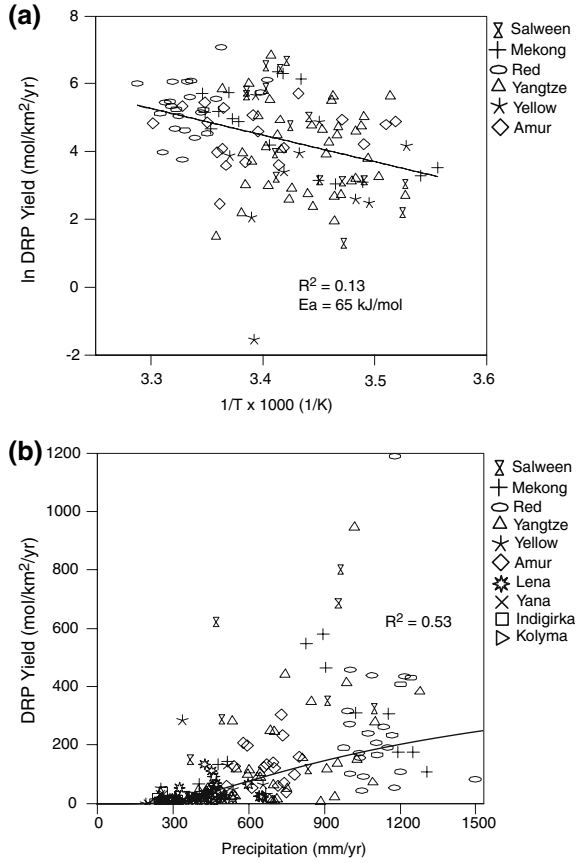

Fig. 7 (**a**) An Arrhenius fit of DRP yield to river water temperature measured in the field. (**b**) A sigmoid fit for DRP yield to precipitation

the activation energy (Koerselman et al. 1993; Guidry and Mackenzie 2003). When the DRP yields of our summer samples were fit to the water temperature measured in the field using an Arrhenius-type function, the correlation coefficient (R^2) was 0.13 (Fig. 7a). The assumption here is that the DRP yield is governed by apatite dissolution whose rate is a function of temperature. The Arrhenius relationship is commonly used to describe the effect of temperature on silicate weathering rates, with the understanding that this can only be an empirical description tool when applied to watershed fluxes involving multiple mineral dissolution reactions and complex hydrochemical processes (White and Blum 1995). This indicated that the variation in water temperature can explain only ~13% of variance in DRP yields. We found only a weak linear correlation between DRP yield and annual precipitation

(R^2 = 0.32) or annual runoff (R^2 = 0.33) for all summer samples excluding those with concentrations <0.06 μM. Fitting to a sigmoid function improved the fit for annual precipitation (R^2 = 0.53, Fig. 7b) though not for annual runoff (R^2 = 0.12). The premise for adopting a sigmoid function was that when rainfall is low, the DRP yield would increase slowly with increasing precipitation, more rapidly at higher rainfall, and reach a plateau in high precipitation systems when the mobile P pool had been exhausted (Harrison et al. 2005).

For the Mekong and Red rivers, both summer and winter samples were available for the same locations. This enabled us to isolate the effect of seasonal climate from that of lithology. Paired-samples *t*-test on 27 summer–winter paired samples showed that the DRP concentrations were higher during the summer high stage than in winter at a 1% significance level. The mean concentration in summer was about 50% higher than that in winter, and the DRP yields (mol DRP/km^2/month) in summer were about four times that in winter. This suggested that the Mekong and Red basins that we sampled were transport-limited systems and that the DRP flushed out with higher supply of water. There were five exceptions: two Mekong tributaries (RD122/RD220 and RD124/RD221) and three from the Red River basin (RD112/RD212, RD108/RD207, and RD118/RD215), having slightly lower concentrations in summer. Major elements Na and Cl in four out of these five rivers showed similar patterns of lower concentrations in summer, which indicated a dilution effect during high water stage.

A stepwise multiple regression using DRP yield, river water temperature, monthly precipitation, monthly evapotranspiration, and monthly runoff on the 54 summer–winter samples resulted in a correlation between DRP yield and precipitation (R^2 = 0.38) at a 5% significance level. Adding parameters such as water temperature, evaporation and runoff did not explain the variance in the DRP yields better than fitting with precipitation alone, probably because the other parameters were strongly correlated with precipitation (R^2 > 0.8).

Anthropogenic impact

According to global P models, approximately 35% of global dissolved inorganic phosphorus export was from natural weathering and 65% from anthropogenic

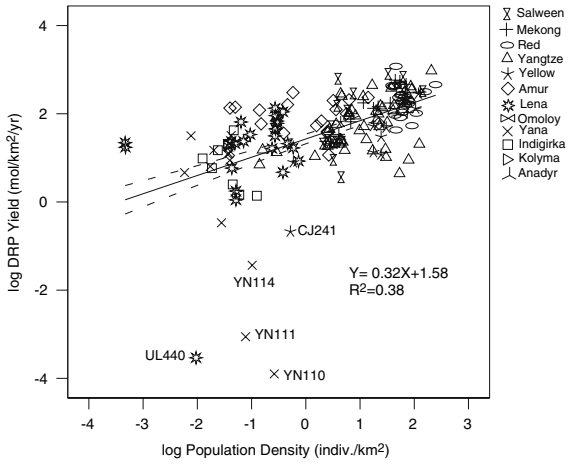

Fig. 8 Relationship between DRP yields and population density in river basins Salween, Mekong, Red, Yangtze, Yellow, Amur, Lena, Omoloy, Yana, Indigirka, Kolyma, and Anadyr. The population densities are for individual sample sub-basins. The dashed lines indicate 95% confidence interval for the regression line. Outliers were excluded when calculating the best-fit equation and R^2 value

(Caraco, 1995; Smith et al. 2003; Harrison et al. 2005). Anthropogenic DRP is mainly from human sewage point sources but could also come from agriculture and fertilizer input. According to Collins and Jenkins (1996), agriculture did not have a big impact on riverine DRP concentration in the Himalayas and may not in our case as well, because the added P was absorbed onto soils or utilized by biota and relatively little was lost to rivers. The DRP concentrations and yields of rivers studied here were in the range of unpolluted major rivers of the world and characteristic of limited human impact (e.g., the Upper Yukon; 12 mol DRP/km^2/year; Guo et al. 2004; Table 1). In contrast, the Seine Basin in France had a DRP yield of 1,700–2,400 mol/km^2/year (Sferratore et al. 2005).

As a quantitative measure of anthropogenic activity, we examined DRP as a function of population density. The population density in our drainage basins was generally low, especially for the East Siberian rivers (Lena, Omoloy, Yana, Indigirka, Kolyma, and Anadyr) (Table 1, Fig. 8). The Red River basin had the highest population density which may have contributed to the generally high DRP in the river (Figs. 4, 5). The Upper Yangtze and Yellow rivers had <20% of the population density of the entire basins (12 vs. 220 per km^2 for the Yangtze, 24

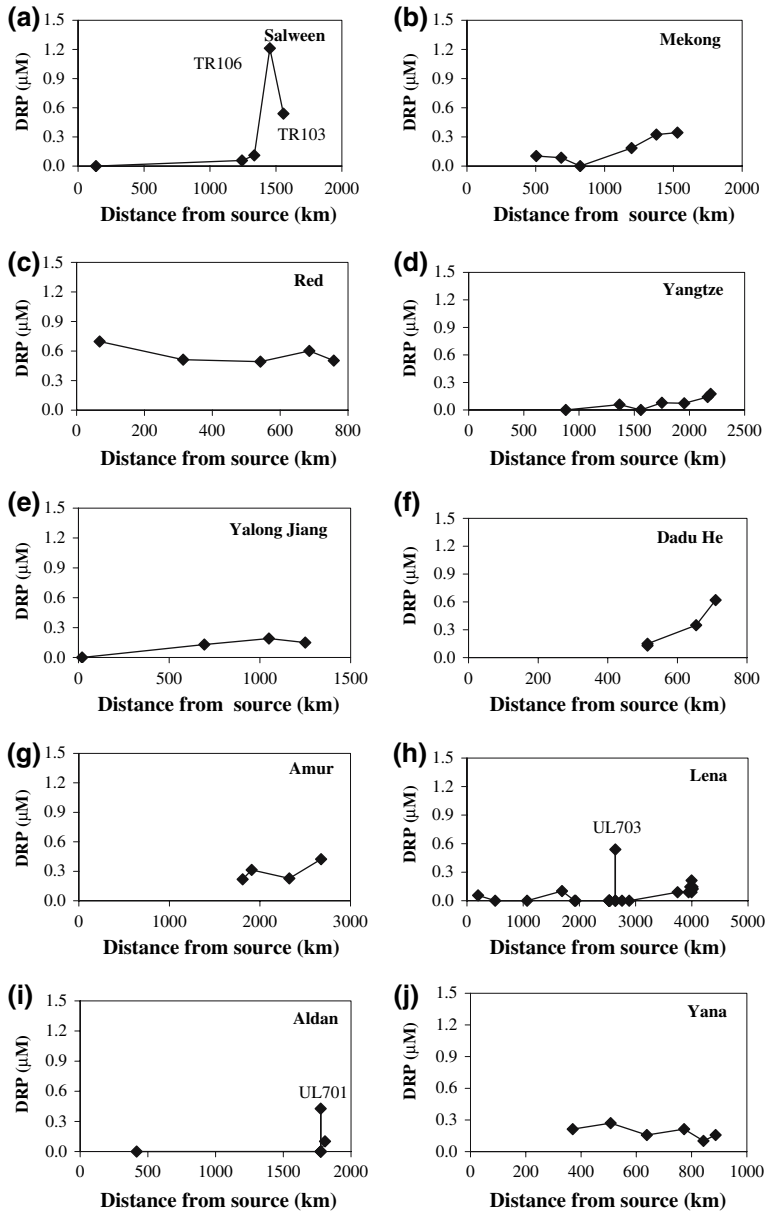

Fig. 9 Downstream evolution of DRP in the main channels where more than three main channel samples were available. Multiyear samples at the same location and summer high water stage samples are included. Yalong Jiang and Dadu He are major left bank tributaries of the Upper Yangtze

vs. 140 per km^2 for the Yellow) (Harrison et al. 2005). When only the outlier samples with high DRP concentrations (Fig. 4) were used for regression, they showed corresponding high population density ($R^2 = 0.55$), although the correlation was poorer between DRP yield outliers (Fig. 5) and population density ($R^2 = 0.40$). The two correlations were significant at a 1% level. Thus, these outliers may be caused by pollution from human sewage point sources. When we considered the full dataset (all rivers at high water stage), the population density can explain 32% of the variance in the DRP concentrations and 38% of the DRP yield variations when excluding outliers (Fig. 8).

Supporting qualitative evidence of anthropogenic effect came from the examination of the downstream evolution of DRP concentrations (Fig. 9). For rivers where we had samples at multiple locations along the main channel, the DRP varied within a narrow range (0.3 μM) except for occasional outliers—Salween

(TR106, TR103), Lena (UL703, UL701). Judging from the fact that (1) the DRP dropped upstream and downstream, (2) sample locations were close to towns or cities, and (3) where multiple year samples were available it was seen for only one year, we considered the outliers to be related to human sewage point source.

There are several within-river processes by which DRP can be modified gradually downstream—biological assimilation, sorption/desorption on sediments, and coprecipitation with calcite (Taylor and Kunish 1971; House et al. 1995; House and Denison 1998; House 2003). The relatively homogeneous variation of main channel values and the short residence time in river water compared to lakes, reservoirs, and stagnant bodies of water, did not permit us to distinguish within-river processes from input/output of P. The low variability downstream of DRP values could also be due to the buffering mechanism by sorption/desoprtion of P onto suspended sediments, especially ferric hydroxide or calcium phosphate type minerals or organic debris (Fox 1989, 1993). Calculation by the Geochemist's Workbench showed that all the river samples are supersaturated with respect to hydroxyapatite. There were five pairs of samples from above and below five different dams or reservoirs (Fig. 10). There was no consistent trend in DRP associated with the reservoirs suggesting that for the spatial and temporal scale of our study, loss mechanisms such as biogenic uptake of P in stagnant waters or sorption onto settling suspended sediments did not appreciably alter downstream transport of DRP.

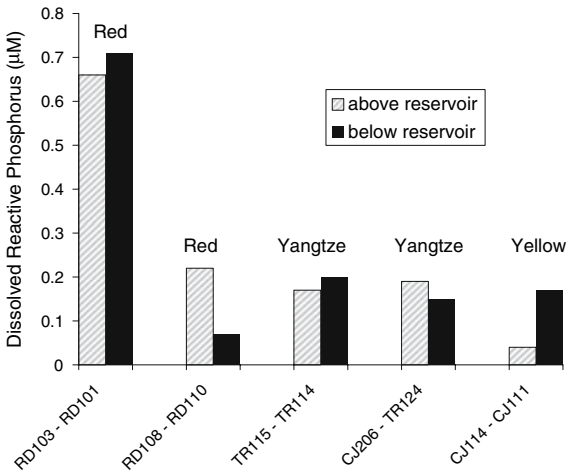

Fig. 10 Bar graph comparing DRP concentrations above and below five dams/reservoirs

We considered the DRP yield, annual precipitation, annual runoff, relief and population density together using stepwise regression for all the summer samples including below detection limit ones. Although DRP yields from summer samples tended to overestimate the annual values, it would not affect our regression result assuming the DRP yield in summer was higher than that in winter in the same magnitude for all the river basins in East Asia. The result showed that annual precipitation was the most important parameter which can explain 37% of the variance in DRP yields; if adding population density to the linear model, 44% of the yield variance could be explained and 48% could be explained if three parameters (precipitation, population density, and runoff) were included in the model.

Conclusions

Dissolved reactive phosphorus concentrations have been determined in large pristine rivers flowing into the Arctic Ocean (the Lena, Omoloy, Yana, Indigirka, and Kolyma rivers) and into the Pacific and Indian Oceans (the Anadyr, Amur, Yellow, Yangtze, Red, Mekong, and Salween). Our results showed that these rivers had relatively low and homogeneous concentrations of DRP in the range of what is considered ''natural'' or ''pristine'' rivers. The outliers with significantly higher concentrations have likely been affected by point sources of human sewage. The high DRP concentration and yield of the Red River can be attributed to the high population density and high precipitation, and there was no direct evidence that the Lao Cai phosphorite deposit contributed to the high levels of DRP in the river. The low mouth values of the East Siberian rivers were due to multiple factors, e.g., low precipitation and sparse population density. The Upper Salween, Mekong, Yangtze and Yellow rivers originating from the Tibetan Plateau supplies 6.1×10^7 mol DRP/year to the Indian and Pacific oceans. The inter-annual variation for DRP concentrations can be up to 1 order of magnitude based on 13 locations sampled in multiple years, implying both human sewage point sources and non-point sources varying as a function of climate and

inputs. Statistical analyses indicated DRP concentrations best related with dissolved Si and K and DRP yield with precipitation and population density. Lithology and relief did not have significant relationships with DRP concentrations and yields perhaps because apatite distribution is relatively uniform across different geological formations. For rivers with seasonal samples, DRP yield in summer was about four times higher than in winter. Our results showed the importance of precipitation among climatic parameters and population density in controlling the riverine DRP yields. This supported the adoption of parameters of runoff and population density in models of the P cycle (e.g., Caraco 1995; Harrison et al. 2005).

Acknowledgments We acknowledge NSF grant EAR-0134966 to Y.H. and Northwestern Alumnae Grant for purchase of UV–Vis spectrometer. For logistical support we thank the River Navigation Authority of Yakutia and A. Zaitsev in Siberia, Chengdu Institute of Geology and J. Qin in China, and V. P. Nguyen in Vietnam. UROP students at MIT, Northwestern, and SNU are thanked for their help in the lab, and we are grateful for discussion and data sharing of J. Borges, A. Ellis, S. Moon, and H. Noh. We thank T. Hare at USGS and P. Reich at USDA for the help with GIS datasets. The thoughtful and thorough review by an anonymous reviewer greatly improved the quality of the paper.

Appendix

Table A1 The location, water discharge, dissolved reactive phosphorus (DRP) concentrations and the P_2O_5 content in bed sediments of the Salween, Mekong, Red, Yangtze, and Yellow river samples

River name*	Sample ID	Date dd–mm–yy	Latitude, degree	Longitude, degree	Discharge, m^3/s	DRP (PO_4), μM	P_2O_5, wt%
Salween							
Salween hw into Cuo Na Lake nr. Amdo	CJ235	14–06–00	91.75	32.22	3.23	b.d.	–
Na Chu @ Na Chu	CJ234	14–06–00	92.03	31.46	2.00	0.07	–
Xiachiu Chu	CJ233	12–06–00	92.79	31.72	28.2	0.08	–
LB trib. of Zi Chu @ Suo Xian	CJ230	11–06–00	93.84	31.92	20.5	b.d.	–
Zi Chu @ Suo Xian	CJ231	11–06–00	93.79	31.89	53.5	b.d.	–
RB trib. of Zi Chu bl. Suo Xian	CJ232	12–06–00	93.72	31.76	5.62	b.d.	–
RB trib. of Rongbu	CJ228	10–06–00	94.64	31.57	4.99	0.07	–
LB trib. of Rongbu	CJ229	10–06–00	94.68	31.57	5.05	0.42	–
LB trib of Salween 4	CJ227	10–06–00	95.11	31.60	14.7	b.d.	–
LB trib of Salween 3	CJ226	10–06–00	95.06	31.62	19.3	0.06	–
LB trib of Salween 2	CJ225	09–06–00	95.78	31.30	12.6	0.07	0.06
LB trib of Salween 1	CJ224	09–06–00	95.88	31.26	8.35	b.d.	0.09
Yu Chu @ Zuo Gong	CJ219	06–06–00	97.89	29.63	55.0	0.08	0.08
Salween bl. Gongshan	TR109	07–08–04	98.70	27.70	1,153	0.06	0.08
LB trib. of Salween	TR108	07–08–04	98.70	27.70	4.70	0.10	0.14
Salween ab. Fugong	TR107	07–08–04	98.87	26.93	1,267	0.11	0.12
Salween ab. Liuku	TR106	07–08–04	98.84	25.90	1,429	1.21	0.09
Laowo He ab. Liuku	TR110	08–08–04	98.87	25.85	20.3	0.32	0.21
RB trib. of Salween @ Manbao	TR105	06–08–04	98.86	25.75	3.09	0.60	0.11
RB trib. of Salween ab. Manyun	TR104	06–08–04	98.87	25.58	1.34	0.55	–
Salween ab. Daojie	TR103	06–08–04	98.87	25.00	1,557	0.54	0.09
Nanding He bl. Lin Cang	RD224	10–01–03	100.10	23.95	0.49	0.27	0.11
Nanding He ab. Yang Tou Yan	RD127	10–09–01	100.04	24.18	0.90	0.45	–
Mekong							
Ang Chu	CJ222	08–06–00	97.09	31.19	4.28	b.d.	0.01
Mekong ab. Bu Chu	CJ221	07–06–00	97.34	30.84	13.0	0.10	–

Table A1 continued

River name*	Sample ID	Date dd–mm–yy	Latitude, degree	Longitude, degree	Discharge, m^3/s	DRP (PO_4), μM	P_2O_5, wt%
Bu Chu hw ab. Lei Wu Chi	CJ223	09–06–00	96.61	31.28	0.77	0.10	0.08
Bu Chu	CJ220	07–06–00	97.30	30.84	1.62	0.09	–
Mekong @ Ru Mei	CJ217	06–06–00	98.34	29.61	18.1	0.09	–
RB trib. of Mekong ab. Ru Mei	CJ218	06–06–00	98.26	29.54	0.30	0.08	–
Mekong ab. Deqen	TR118	11–08–04	98.82	28.47	20.0	b.d.	–
Caojian He ab. Wayao	TR111	09–08–04	99.22	25.48	0.29	0.63	–
Mekong	TR112	09–08–04	99.29	25.39	33.2	0.19	0.10
Yangbi Jiang @ Pinpo	TR101	05–08–04	100.05	25.59	4.17	0.58	–
Shunbi He	TR102	05–08–04	99.97	25.49	1.25	0.80	0.05
Mekong ab. Noja He	RD129	10–09–01	100.44	24.64	44.9	0.32	–
Mekong ab. Noja He	RD227	11–01–03	100.44	24.64	44.9	b.d.	–
Noja He	RD128	10–09–01	100.47	24.52	1.62	0.56	0.15
Noja He	RD226	11–01–03	100.47	24.52	1.62	0.49	0.28
RB trib. of Mekong	RD225	10–01–03	100.29	24.09	0.29	0.25	0.11
Mekong @ Da Hai	RD126	09–09–01	100.18	23.56	49.3	0.34	–
Mekong @ Da Hai	RD223	09–01–03	100.18	23.56	49.3	0.08	0.09
Mongga He	RD125	09–09–01	100.30	23.60	1.07	0.23	0.04
Mongga He	RD222	09–01–03	100.30	23.60	1.07	0.06	–
Weiyuan Jiang @ Jing Gu	RD124	08–09–01	100.71	23.50	1.90	0.45	–
Weiyuan Jiang @ Jing Gu	RD221	08–01–03	100.71	23.50	1.90	0.48	–
Xiaohei Jiang	RD122	08–09–01	100.93	23.21	0.33	0.16	0.05
Xiaohei Jiang	RD220	08–01–03	100.93	23.21	0.33	0.26	0.05
TyeYangtze	RD123	08–09–01	100.93	23.21	0.77	0.24	0.04
TyeYangtze	RD219	08–01–03	100.93	23.20	0.77	0.16	0.08
Red (Hong He)							
Da							
Amo Jiang	RD120	07–09–01	101.51	23.35	1.68	2.60	0.07
Amo Jiang	RD217	07–01–03	101.51	23.35	1.68	0.33	–
Babian Jiang	RD121	07–09–01	101.33	23.24	2.98	0.49	0.07
Babian Jiang	RD218	07–01–03	101.33	23.24	2.98	0.25	0.07
Da @ Lai Chau	RD105	19–08–01	103.16	22.08	14.3	0.79	–
Da @ Lai Chau	RD203	29–12–02	103.16	22.08	14.3	0.49	0.06
Namna @ Lai Chau	RD104	19–08–01	103.16	22.08	0.92	0.82	–
Namna @ Lai Chau	RD204	29–12–02	103.16	22.08	0.92	0.66	0.11
Da @ Muong La, ab. res.	RD103	18–08–01	104.04	21.46	26.7	0.66	0.08
Da @ Muong La, ab. res.	RD202	28–12–02	104.04	21.46	26.7	0.48	0.07
Trib. of Da @ Yen Chau	RD102	17–08–01	104.36	21.03	0.39	0.17	–
Da @ Hoa Binh, bl. res.	RD101	17–08–01	105.36	20.83	30.8	0.71	–
Da @ Hoa Binh, bl. res.	RD201	27–12–02	105.36	20.83	30.8	0.28	–
Red Main Channel							
Upper Lishe Jiang, LB	RD131	11–09–01	100.55	25.09	0.45	0.89	–
Upper Lishe Jiang, LB	RD229	12–01–03	100.55	25.09	0.45	0.27	–
Upper Lishe Jiang, RB	RD130	11–09–01	100.53	25.06	0.73	0.70	–

Table A1 continued

River name*	Sample ID	Date dd–mm–yy	Latitude, degree	Longitude, degree	Discharge, m^3/s	DRP (PO_4), μM	P_2O_5, wt%
Upper Lishe Jiang, RB	RD228	12–01–03	100.53	25.06	0.73	0.25	–
Red @ Yuan Jiang	RD119	05–09–01	101.98	23.63	7.09	0.51	0.12
Red @ Yuan Jiang	RD216	06–01–03	101.98	23.63	7.09	0.40	–
Huanien He	RD118	05–09–01	102.17	23.88	0.16	0.27	–
Huanien He	RD215	06–01–03	102.17	23.88	0.16	0.35	–
Red @ Cua Khao, nr. Lao Cai	RD106	22–08–01	103.85	22.59	11.1	0.49	–
Red @ Cua Khao, nr. Lao Cai	RD205	30–12–02	103.85	22.59	11.1	0.24	0.10
Nanxi	RD117	04–09–01	103.88	22.68	1.15	0.46	–
Xiaonanxi	RD116	04–09–01	103.94	22.65	0.18	0.14	–
Namthe @ Lao Cai	RD107	22–08–01	104.01	22.52	0.25	0.58	–
Namthe @ Lao Cai	RD206	31–12–02	104.01	22.52	0.25	0.48	0.20
Red @ Yen Bai	RD109	23–08–01	104.84	21.74	20.7	0.60	–
Red @ Yen Bai	RD208	31–12–02	104.84	21.74	20.7	0.39	0.08
Red @ Phu Tho	RD115	26–08–01	105.23	21.40	22.8	0.50	–
Red @ Phu Tho	RD214	02–01–03	105.23	21.40	22.8	0.46	0.10
Lo							
Lo @ Ha Jiang	RD111	24–08–01	104.98	22.84	3.41	0.21	0.10
Lo @ Ha Jiang	RD211	01–01–03	104.98	22.84	3.41	0.18	–
Con @ Vinh Tuy	RD112	25–08–01	104.89	22.27	1.01	0.13	–
Con @ Vinh Tuy	RD212	02–01–03	104.89	22.27	1.01	0.20	–
Gam @ Chiem Hoa	RD113	25–08–01	105.28	22.14	3.33	0.31	–
Gam @ Chiem Hoa	RD210	01–01–03	105.28	22.14	3.33	0.22	0.09
Chay @ Bao Yen	RD108	22–08–01	104.48	22.24	0.31	0.22	–
Chay @ Bao Yen	RD207	31–12–02	104.48	22.24	0.31	0.24	0.09
Chay @ Doan Hung, bl. Thac Ba res.	RD110	23–08–01	105.08	21.72	1.73	0.07	–
Chay @ Doan Hung, bl. Thac Ba res.	RD209	01–01–03	105.08	21.72	1.73	0.07	0.02
Lo @ Doan Hung, bl. Chay	RD114	26–08–01	105.19	21.62	1.94	0.27	–
Lo @ Doan Hung, bl. Chay	RD213	02–01–03	105.19	21.62	1.94	0.22	0.09
Yangtze (Chang Jiang)							
Bu Chu	CJ236	15–06–00	92.35	33.83	26.1	0.11	–
Neier Chu	CJ237	15–06–00	92.29	33.86	15.3	0.06	0.07
Tuotuo He	CJ238	15–06–00	92.47	34.22	51.4	0.19	–
Chumaer He @ Chu Ma Er Hei Yen	CJ239	16–06–00	93.31	35.31	0.70	b.d.	0.04
Jinsha Jiang @ Zi Men Xia	CJ118	02–06–99	97.22	33.03	396	b.d.	0.06
RB trib. of Jinsha Jiang @ Yu Shu	CJ119	02–06–99	97.11	33.00	19.7	0.06	–
LB trib. of Batang	CJ213	03–06–00	99.51	30.28	1.18	0.06	–
Batang	CJ214	05–06–00	99.08	29.97	39.3	0.06	–
Jinsha Jiang @ Zhu Ba Long	CJ215	05–06–00	99.01	29.79	928	0.06	–
RB trib. of Jinsha Jiang	CJ216	05–06–00	98.97	29.76	31.4	0.06	–
Gangqu He	TR116	11–08–04	99.39	28.18	30.3	0.06	–
Jinsha Jiang	TR117	11–08–04	99.38	28.18	1,240	b.d.	0.08

Table A1 continued

River name*	Sample ID	Date dd–mm–yy	Latitude, degree	Longitude, degree	Discharge, m^3/s	DRP (PO_4), μM	P_2O_5, wt%
Jinsha Jiang bl. Hutiao Xia	TR113	10–08–04	100.05	27.13	1,444	0.08	–
Xiaozhongdian He ab. dam	TR115	10–08–04	99.99	27.32	43.0	0.17	–
Xiaozhongdian He	TR114	10–08–04	100.06	27.18	47.3	0.20	–
Jinsha Jiang @ Jin An Qiao	TR119	13–08–04	100.43	26.82	1,853	0.07	–
LB trib. of Jinsha Jiang	TR120	13–08–04	100.46	26.79	18.5	0.53	–
Maguo He	TR121	14–08–04	101.03	26.44	14.1	0.37	0.17
Tongda He @ Shilong Ba	TR122	14–08–04	101.34	26.59	7.86	1.68	–
Jinsha Jiang @ Geli Ping	TR123	14–08–04	101.53	26.59	2,209	0.14	0.13
Jinsha Jiang bl. Panzhi Hua	TR126	15–08–04	101.78	26.60	42.8	0.18	0.16
Yalong Jiang nr. Chingshui He	CJ117	02–06–99	97.17	33.73	17.7	b.d.	–
Yalong Jiang @ Manigango	CJ123	03–06–99	99.45	31.80	31.7	0.09	–
Ni Chu ab. Da Wu	CJ126	05–06–99	101.07	31.03	226	b.d.	0.13
LB trib. of Ya Jiang	CJ210	02–06–00	101.20	30.07	8.69	0.26	–
Ya Jiang	CJ211	02–06–00	101.02	30.03	981	0.13	–
Litang	CJ212	03–06–00	100.19	29.98	32.2	0.53	–
Yalong Jiang	CJ206	29–05–00	101.88	28.32	2,104	0.19	0.10
Yalong Jiang bl. Er Tan dam	TR124	15–08–04	101.80	26.81	2,220	0.15	–
Anning	CJ205	29–05–00	102.19	28.56	29.9	0.15	–
Anning ab. Yalong Jiang	TR125	15–08–04	101.87	26.73	201	0.61	–
Longchuan Jiang	RD132	12–09–01	101.57	25.06	25.2	2.11	–
Dadu He nr. Lu Ding	CJ128	06–06–99	102.23	29.93	1,262	0.13	–
Dadu He nr. Lu Ding	CJ209	01–06–00	102.23	29.93	1,288	0.15	–
Shimian	CJ207	29–05–00	102.40	29.20	25.2	0.23	0.04
Dadu He	CJ204	28–05–00	102.83	29.22	1,487	0.35	0.18
Niri He	CJ203	28–05–00	102.85	29.18	102	0.37	0.17
RB trib. of Dadu He	CJ202	28–05–00	103.20	29.21	40.0	0.43	–
Dadu He ab. Ebian	CJ201	27–05–00	103.24	29.25	1,653	0.62	–
Ching Jiang @ Tien Chuan	CJ208	01–06–00	102.76	30.06	50.8	0.09	0.12
Fou Jiang ab. Ping Wu	CJ103	28–05–99	104.59	32.39	49.6	b.d.	0.02
Bailong Jiang @ Liang He Kou	CJ138	14–06–99	104.45	33.70	116	b.d.	–
Bailong Jiang LB trib. @ Liang He Kou	CJ139	14–06–99	104.50	33.72	8.49	b.d.	–
Wun Jiang	CJ136	12–06–99	105.02	32.83	50.9	0.08	–
Bailong Jiang @ Yao Tu	CJ135	12–06–99	105.42	32.78	180	0.08	–
RB trib. of Jialing Jiang	CJ132	11–06–99	105.66	32.40	181	0.33	–
Chingjiang He	CJ131	11–06–99	105.54	32.30	4.18	0.09	–
Jialing Jiang @ Feng Xian	CJ145	14–06–99	106.47	33.90	2.24	0.25	–
Jialing Jiang	CJ134	12–06–99	105.83	32.46	24.0	0.31	–
Xi He @ Mu Rhen	CJ130	11–06–99	105.28	31.87	0.48	0.55	–
LB trib. of Han Shui	CJ146	15–06–99	106.95	33.25	28.7	0.22	–
Yellow (Huang He)							
Yellow @ Ma Doi	CJ116	02–06–99	98.15	34.90	61.1	b.d.	–
Mo Chu @ Roergai	CJ107	30–05–99	102.92	33.60	36.1	0.16	–
Yellow bl. Tangnag	CJ114	01–06–99	100.25	35.68	876	b.d.	0.02

Table A1 continued

River name*	Sample ID	Date dd–mm–yy	Latitude, degree	Longitude, degree	Discharge, m^3/s	DRP (PO_4), μM	P_2O_5, wt%
Tao He @ Min Xian	CJ141	14–06–99	104.02	34.43	127	b.d.	–
Tao He ab. Lin Tao	CJ247	21–06–00	103.85	35.34	152	0.20	–
Datong He @ Min He	CJ112	31–05–99	102.83	36.38	41.2	0.15	–
Datong He @ Min He	CJ244	20–06–00	102.83	36.38	41.2	0.60	–
Huang Shui ab. Min He	CJ245	20–06–00	102.75	36.33	33.4	4.12	–
Yellow @ Lanzhou	CJ111	31–05–99	103.52	36.13	1264	0.17	–
Yellow @ Lanzhou	CJ246	20–06–00	103.52	36.13	1264	0.17	–
Wei He @ Wu Shan	CJ142	15–06–99	104.87	34.73	17.0	1.98	0.11
Nachiguole	CJ240	16–06–00	94.79	35.93	–	0.08	0.12
Goldmud	CJ241	17–06–00	94.83	35.93	0.84	0.09	–
Qaidam @ Xiangride	CJ242	17–06–00	97.87	36.00	46.7	0.07	0.10

*hw., bl., ab., nr., res., trib. denote headwater, below, above, near, reservoir, tributary; – denotes unavailable discharge data or bed sediment samples; b.d. = below detection limit (0.06 μM)

Dissolved major elements and Sr isotope data for these samples are in Moon et al. (2007), Noh et al. (in prep), Ellis et al. (in prep), and Wu et al. (2005)

Table A2 The location, water discharge, dissolved reactive phosphorus (DRP) concentrations and the P_2O_5 content in bed sediments of the East Siberian rivers*

River name	Sample ID	Date dd–mm–yy	Latitude, Degree	Longitude, Degree	Discharge, m^3/s	DRP (PO_4), μM	P_2O_5, wt%
Amur							
Tom	AU114	15–07–98	50.93	128.43	116	0.48	–
Belaya @ bridge	AU113	15–07–98	50.67	128.08	9.11	1.16	–
Ivanovka	AU112	15–07–98	50.37	128.00	4.58	1.37	–
Zeya	AU115	16–07–98	50.28	127.57	2,006	0.20	–
Amur @ Heihe	AU116	16–07–98	50.25	127.48	1,071	0.22	–
Amur @ Konstantinovka	AU111	13–07–98	49.58	127.93	3,507	0.31	–
Bureya	AU117	18–07–98	49.45	129.50	982	0.08	–
Hingan	AU109	10–07–98	48.88	130.63	27.2	0.16	–
Mutnaya	AU110	10–07–98	48.88	130.60	10.2	0.70	–
Dichun	AU108	09–07–98	48.52	130.73	4.35	0.31	–
Pompeyevka	AU107	09–07–98	48.35	130.82	6.05	0.44	–
Tulovchikha	AU106	09–07–98	48.08	130.67	1.15	0.48	–
Amur ab. Amurzet	AU105	08–07–98	47.90	130.90	5,093	0.23	–
Bidzhan	AU104	07–07–98	47.95	132.07	64.9	0.23	–
Sungari	AU118	20–07–98	47.75	132.58	1,914	1.20	–
Bira	AU103	06–07–98	48.18	133.25	119	0.28	–
Amur ab. Khabarovsk	AU102	05–07–98	48.43	134.88	7,291	0.42	–
Ussuri	AU119	23–07–98	48.33	134.83	1,909	0.75	–
Tunguska	AU101	04–07–98	48.60	134.95	416	0.37	–
Lena							
Manzurka	UL401	24–07–94	53.74	106.02	1.28	b.d.	–
Lena ab. Manzurka	UL402	24–07–94	53.86	106.24	22.6	0.06	–

Table A2 continued

River name	Sample ID	Date dd–mm–yy	Latitude, Degree	Longitude, Degree	Discharge, m^3/s	DRP (PO_4), μM	P_2O_5, wt%
Tutura	UL403	25–07–94	54.79	105.21	70.0	0.11	–
Lena ab. Orlinga	UL405	26–07–94	55.98	105.86	135	b.d.	0.11
Orlinga	UL404	26–07–94	56.08	105.84	176	b.d.	–
Kuta	UL408	27–07–94	56.72	105.63	225	b.d.	–
Tayura	UL407	27–07–94	56.98	106.59	48.6	b.d.	0.11
Bolshaya Tira	UL409	28–07–94	57.31	107.23	15.0	b.d.	–
Ulkan	UL410	28–07–94	57.25	107.24	365	b.d.	–
Well @ Kirensk	UL411	26–07–94	57.57	107.70	379	b.d.	–
Mogol	UL415	31–07–94	56.73	107.96	446	b.d.	0.11
Kutima, trib. of Kirenga	UL414	31–07–94	57.12	108.29	26.66	b.d.	–
Kirenga	UL413	30–07–94	57.42	107.97	516	b.d.	–
Nizhnyaya Tunguska	UL412	29–07–94	58.08	108.03	8.12	b.d.	–
Chaya	UL416	02–08–94	58.22	109.57	58.4	b.d.	0.06
Lena ab. Ichera	UL417	02–08–94	58.31	109.66	987	b.d.	–
Melnichnui Creek	UL418	02–08–94	58.45	109.74	988	b.d.	–
Spring	UL419	02–08–94	58.57	109.90	989	0.09	–
Ichera	UL420	02–08–94	58.58	109.72	2.84	b.d.	–
Chuya	UL421	02–08–94	59.23	112.39	133	b.d.	–
Mama, trib. of Vitim	UL422	03–08–94	58.14	113.38	14.2	b.d.	–
B. Severnaya, trib. of Vitim	UL424	04–08–94	58.16	112.91	172	b.d.	–
Maximikha, trib. of Vitim	UL425	04–08–94	58.33	112.87	1,831	b.d.	0.10
Vitim bl. Mama	UL423	04–08–94	58.49	112.96	5.66	b.d.	–
Barchikha, trib. of Vitim	UL426	04–08–94	58.71	113.02	9.39	0.08	–
V. Yzobaya, trib. of Vitim	UL427	04–08–94	58.89	112.98	7.71	0.08	–
N. Yzobaya, trib. of Vitim	UL428	04–08–94	58.99	112.83	4.70	0.08	–
Peleduy	UL429	05–08–94	59.67	112.69	66.2	b.d.	–
Pulka	UL430	06–08–94	60.11	113.96	12.8	0.08	–
Khamra	UL431	06–08–94	60.25	114.09	14.2	b.d.	0.14
Nyuya	UL432	07–08–94	60.63	116.34	114	b.d.	–
Ura	UL433	07–08–94	60.47	116.77	0.24	b.d.	0.04
Lena ab. Bolshoy Patom	UL716	08–08–96	60.12	117.10	3,257	0.10	–
B. Patom	UL434	07–08–94	60.02	116.99	174	b.d.	0.10
B. Patom	UL715	08–08–96	60.02	116.99	174	b.d.	–
M. Patom	UL435	07–08–94	59.89	117.34	10.7	b.d.	–
M. Patom	UL714	08–08–96	59.89	117.34	10.7	b.d.	–
Biryuk	UL436	08–08–94	60.33	119.57	0.27	b.d.	–
Biryuk	UL713	07–08–94	–	–	–	b.d.	–
Lena @ Olekminski	UL439	09–08–94	60.44	120.12	–	b.d.	–
Lena @ Olekminsk, ab. Olekma & Chara	UL712	07–08–97	60.33	120.22	3,435	b.d.	–
Chara	UL437	08–08–94	60.20	121.02	688	0.14	0.12
Chara	UL710	05–08–92	60.20	121.02	688	b.d.	–
Olekma	UL438	08–08–94	60.21	121.16	1,578	b.d.	0.11
Olekma	UL711	06–08–94	60.21	121.16	1,578	b.d.	–
Namana	UL440	10–08–94	60.68	121.14	–	0.14	0.03

Table A2 continued

River name	Sample ID	Date dd–mm–yy	Latitude, Degree	Longitude, Degree	Discharge, m^3/s	DRP (PO_4), μM	P_2O_5, wt%
Tuolbachen	UL204	03–08–92	60.49	122.87	11.2	b.d.	0.04
Tuolbachen	UL441	11–08–94	60.49	122.87	11.2	b.d.	–
Tuolbachen	UL709	05–08–96	60.49	122.87	11.2	b.d.	–
Markha	UL442	11–08–94	60.66	123.17	2.24	0.14	–
Markha	UL708	05–08–96	60.66	123.17	2.24	0.21	–
Markhachan	UL443	12–08–94	60.62	123.54	4.15	0.19	–
Tuolba	UL444	12–08–94	60.58	124.32	139	0.08	–
Tuolba	UL707	05–08–96	60.58	124.32	139	b.d.	–
Malykhan	UL445	13–08–94	60.66	124.57	5,823	0.30	–
Malykhan	UL706	05–08–96	60.66	124.57	5,823	0.27	–
R.B. stream opposite Malykhan	UL445–1	13–08–94	60.76	124.65	–	0.08	–
Sinyaya	UL205	03–08–92	61.23	126.91	8.33	b.d.	0.03
Buotama	UL705	04–08–96	61.41	129.01	5,898	0.43	–
R.B.Spring bl.Buotama	UL704	03–08–96	61.41	129.01	5,898	0.21	–
Lena ab. Yakutsk	UL446	14–08–94	–	–	–	b.d.	–
Lena ab. Yakutsk	UL206	04–08–92	61.94	129.71	5,889	b.d.	–
R.B. Spring bl Orlinga	UL406	26–07–94	61.94	129.71	5,889	b.d.	–
Lena @ Yakutsk, Markha	UL–Chnl1	04–08–92	62.00	129.67	–	b.d.	–
Lena @ Yakutsk, Zhatai	UL–Chnl2	04–08–92	62.00	129.67	–	b.d.	–
Lena @ Yakutsk, Prigorodnyi	UL–Chnl3	04–08–92	62.00	129.67	–	b.d.	–
Lena @ mouth above Aldan	UL102	27–07–91	62.89	129.77	5,872	b.d.	0.04
Lena @ mouth above Aldan	UL703	31–07–96	62.89	129.77	5,872	0.54	–
Lena @ mouth above Aldan	UL811	03–09–97	62.89	129.77	5,872	b.d.	–
M. Kuranakh, trib. of Aldan	UL807	30–08–97	58.83	125.39	23.0	b.d.	–
Upper Elkon, trib. of Aldan	UL808	30–08–97	58.85	125.48	16.9	b.d.	–
Yakokut, trib. of Aldan	UL120	08–09–91	59.06	125.82	44.5	b.d.	0.10
B. Kuranakh, trib. of Aldan	UL803	29–08–97	–	–	–	b.d.	–
Aldan @ Tommot	UL802	29–08–97	58.89	126.29	17.6	b.d.	–
B. Khatymy, trib. of Timpton	UL805	30–08–97	57.22	125.16	33.3	b.d.	–
B. Nimnyr, trib. of Aldan	UL806	30–08–97	58.04	125.66	53.6	0.07	–
Yllymakh @ village, trib. of Aldan	UL809	30–08–97	58.56	126.60	82.8	b.d.	–
Illymakh	UL118	08–08–91	58.57	126.87	92.8	b.d.	0.15
Sumnagin	UL117	07–08–91	58.87	127.61	32.5	b.d.	–
Ice Field	UL116	07–08–91	58.79	127.99	–	b.d.	0.11
Jelinda	UL115	05–08–91	58.52	128.69	7.60	b.d.	–
Sumnayn	UL114	05–08–91	58.50	128.94	67.2	b.d.	–
Junikan	UL113	04–08–91	58.50	129.31	18.5	b.d.	0.07
Great Seligri	UL112	04–08–91	58.57	130.15	41.7	b.d.	0.05
Uchur	UL110	03–08–91	58.70	130.77	2,284	b.d.	0.02
Maya	UL109	02–08–91	60.35	134.58	1,414	b.d.	0.04
Allakh-Yun	UL123	13–08–91	60.61	135.17	126	b.d.	0.09
Tyry	UL126	15–08–91	62.48	136.04	30.0	b.d.	0.14
East Chandyga	UL107	31–07–91	62.53	135.37	–	b.d.	0.12
Chulman, trib. of Timpton	UL804	30–08–97	59.60	125.02	13.5	b.d.	–

Table A2 continued

River name	Sample ID	Date dd–mm–yy	Latitude, Degree	Longitude, Degree	Discharge, m^3/s	DRP (PO_4), μM	P_2O_5, wt%
Elkon @ mouth, trib. of Aldan	UL121	08–09–91	59.65	127.04	219	b.d.	–
Amga @ Verkhnyaya Amga	UL801	29–08–97	59.66	127.75	301	b.d.	–
Amga	UL106	30–07–91	62.58	135.09	391	b.d.	0.02
Tompo	UL127	15–08–91	62.79	134.83	64.7	b.d.	0.12
Tukulan	UL131	16–08–91	63.38	131.88	26.1	b.d.	0.12
Tamara	UL702	31–07–95	63.42	130.45	25.6	0.54	–
Aldan @ mouth	UL101	26–07–91	63.41	130.04	7,050	b.d.	0.04
Aldan @ mouth	UL203	01–09–92	63.41	130.04	7,050	b.d.	–
Aldan @ mouth	UL701	31–07–96	63.41	130.04	7,050	0.43	–
Aldan @ mouth	UL810	03–09–97	63.41	130.04	7,050	b.d.	–
Aldan @ mouth	UL601	22–07–95	63.47	129.43	7,048	0.10	–
Notora	UL124	14–08–91	63.46	128.82	0.02	b.d.	0.05
Lena bl. Aldan	UL103	28–07–91	63.46	128.59	0.001	b.d.	0.03
Lena ab. Vilyui	UL202	01–09–92	64.22	126.71	0.55	b.d.	–
Vilyuy @ mouth	UL201	01–09–92	63.96	125.91	870	b.d.	0.01
Sobolokh	UL602	23–07–95	67.23	123.54	38.5	b.d.	0.10
Menkere	UL604	24–07–95	68.01	123.32	33.5	b.d.	0.12
Natara	UL605	24–07–95	68.40	123.96	12.2	b.d.	–
Dzhardzhan	UL606	24–07–95	68.73	124.06	14.8	b.d.	0.13
Lena @ Kusur	UL607	25–07–95	70.76	127.52	13,643	0.09	–
Lena @ mouth, Stolb Island	UL614	31–07–95	72.37	126.68	–	0.09	0.03
Small river from a lake	UL613	31–07–95	72.42	126.31	–	0.09	0.03
Lena @ mouth, Olenek Channel	UL609	26–07–95	72.42	125.72	–	0.15	0.06
Lena @ mouth, Tumatskaya Channel	UL610	26–07–95	72.90	126.36	–	0.09	0.07
Lena @ mouth, Trofimovsky Channel	UL611	28–07–95	72.88	127.00	–	0.21	0.04
Lena @ mouth, Bukofsky Channel	UL612	29–07–95	72.56	128.26	–	0.15	–
Ulakhen-Yuryage	UL617	02–08–95	72.50	124.79	–	0.07	–
Kuogastakh–Yuryage	UL619	02–08–95	72.41	125.07	–	0.12	–
Erdilyakh-Yuryage	UL620	02–08–95	72.31	125.45	–	0.07	–
Lena @ mouth, Olenyokskaya Channel, @ Khtyraya	UL618	02–08–95	72.64	124.64	–	0.12	–
Lena @ Yakutsk, Canal	UL-PortCh	04–08–92	62.00	129.67	–	b.d.	–
Lake Baikal @ mouth of Angara River	LB202	24–07–94	–	–	–	b.d.	–
Omoloy							
Turka creek	OM101	21–08–95	70.63	134.13	1.69	b.d.	–
Ekyes	OM102	21–08–95	70.70	134.11	0.63	b.d.	–
Kyugyulyur	OM103	21–08–95	70.66	133.61	1.90	b.d.	–
Omoloy ab. Kyugyulyur	OM104	21–08–95	70.65	133.42	24.6	b.d.	–
Yana							
Sartang	YN111	13–08–95	67.42	133.29	0.0001	0.33	–
Dulgalakh	YN112	13–08–95	67.51	133.08	126	0.21	–
Arga-Bullyakh	YN110	13–08–95	67.49	133.93	0.0001	0.06	–
Yana @head	YN109	13–08–95	67.58	134.26	226	0.21	–
Kytalyktakh	YN113	16–08–95	67.99	134.56	0.01	0.83	–

Table A2 continued

River name	Sample ID	Date dd–mm–yy	Latitude, Degree	Longitude, Degree	Discharge, m^3/s	DRP (PO_4), μM	P_2O_5, wt%
Tuostakh	YN115	17–08–95	67.89	135.78	28.6	0.10	–
Adycha above Tuostakh	YN114	17–08–95	67.80	135.56	151	0.21	–
Adycha @ mouth	YN116	17–08–95	68.20	134.86	179	0.10	–
Oldzan	YN117	18–08–95	68.48	135.18	1.63	0.10	–
Black River	YN118	18–08–95	68.44	134.77	401	0.16	–
Yana bl. Oldzan	YN108	12–08–95	68.67	134.60	401	0.27	–
Yana bl. Dzhangky	YN106	10–08–95	69.79	135.16	527	0.16	–
Yana ab. delta	YN105	09–08–95	70.50	134.87	572	0.21	–
Yana, 154km from mouth	YN104	09–08–95	70.80	136.21	612	0.10	–
Kochevaya channel	YN103	09–08–95	70.92	136.43	–	0.10	–
Kamelyot channel	YN102	09–08–95	71.08	136.29	–	0.10	–
Yana, 47 km from mouth	YN101	08–08–95	71.11	135.99	634	0.16	–
Kava	MD101	09–09–97	–	–	–	b.d.	–
Yana	MD102	09–09–97	–	–	–	b.d.	–
Arman	MD103	09–09–97	–	–	–	b.d.	–
Indigirka							
Moma	IG109	19–07–96	66.27	143.42	205	b.d.	–
Indigirka ab.Moma	IG110	20–07–96	66.37	143.17	731	b.d.	–
Ilin-Eselyakh	IG108	18–07–96	66.67	142.98	4.89	b.d.	–
Syuryuktyakh	IG107	17–07–96	67.03	142.45	14.3	b.d.	–
Jyekhatyekha	IG106	16–07–96	67.16	142.78	0.77	b.d.	–
Kolyadin	IG105	15–07–96	67.45	142.55	0.36	b.d.	–
Indigirka @ Red River	IG103	14–07–96	67.58	143.22	751	b.d.	–
Talbykchan	IG104	14–07–96	67.61	143.31	0.06	0.11	–
Red River	IG102	14–07–96	67.61	143.77	0.05	0.17	–
RB trib. of Indigirka	IG101	13–07–96	67.56	144.57	0.25	0.34	–
Kebergene	IG111	21–07–96	67.72	144.48	0.20	b.d.	–
Selennyakh	IG112	22–07–96	67.86	144.76	21.9	b.d.	–
Bor-Uryakh	IG113	23–07–96	68.17	145.77	3.40	0.06	–
Badyarikha	IG114	23–07–96	68.26	146.14	41.5	0.06	–
Uyandina	IG115	23–07–96	68.44	145.72	208	0.06	–
Suturuokha	IG116	25–07–96	68.56	146.09	28.7	0.06	–
Indigirka ab. Tirekhtyakh	IG118	25–07–96	68.54	146.88	1,096	b.d.	–
Tirekhtyakh	IG117	25–07–96	68.59	147.09	8.96	b.d.	–
Shanguina	IG119	26–07–96	69.08	147.53	44.7	b.d.	–
Bolshaya Ercha	IG120	26–07–96	69.54	147.71	48.4	0.11	–
Indigirka bl. B. Ercha	IG121	26–07–96	69.58	147.58	1,274	0.11	–
Kolyma							
Kolyma ab. Buyunda	KY103	13–08–92	62.62	152.38	1,047	b.d.	–
Buyunda	KY102	13–08–92	62.70	152.73	247	b.d.	–
Seymchan	KY101	13–08–92	63.01	152.29	17.4	b.d.	–
Balygychan	KY104	14–08–92	63.94	154.29	131	b.d.	–
Kolyma ab. Sugoy	KY106	15–08–92	64.15	154.40	1,469	0.07	–
Sugoy	KY105	15–08–92	64.21	154.70	216	b.d.	–

Table A2 continued

River name	Sample ID	Date dd–mm–yy	Latitude, Degree	Longitude, Degree	Discharge, m^3/s	DRP (PO_4), μM	P_2O_5, wt%
Burgali	KY107	15–08–92	64.36	153.96	0.86	0.09	–
Korkodon	KY108	15–08–92	64.79	154.19	143	b.d.	–
Stolbovaya	KY109	15–08–92	64.81	153.77	2.66	b.d.	–
Shamanikha	KY110	16–08–92	65.20	151.88	2.75	b.d.	–
Zyryanka	KY112	17–08–92	65.80	150.71	35.7	b.d.	–
Ozhogina	KY114	18–08–92	66.19	150.94	45.6	b.d.	–
Sepyakine	KY115	19–08–92	66.47	152.00	2.28	b.d.	–
Kamenka	KY116	19–08–92	66.76	152.70	4.09	b.d.	–
Sedjodima	KY117	20–07–92	67.11	152.95	6.75	b.d.	–
Berezovka	KY118	20–08–92	67.50	155.32	4.04	b.d.	–
Omolon	KY119	21–08–92	68.63	158.61	723	b.d.	–
Bolshoy Anyuy	KY122	22–08–92	68.33	160.84	249	b.d.	–
Malyy Anyuy	KY121	22–08–92	68.31	161.21	194	b.d.	–
Kolyma @ mouth	KY120	22–08–92	68.54	161.14	3,192	b.d.	–
Anadyr							
Belaya	AY104	25–08–97	65.63	173.37	231	b.d.	–
Anadyr @ Markhovo	AY109	04–09–97	64.75	170.80	580	b.d.	–
Mayn	AY107	01–09–97	65.02	172.05	390	b.d.	–
Anadyr ab. Mayn	AY108	01–09–97	65.16	172.12	739	b.d.	–
Anadyr ab. Belaya	AY106	28–08–97	65.48	173.02	1,163	b.d.	–
Anadyr ab. Tanyurer	AY103	24–08–97	64.86	174.07	1,440	b.d.	–

*b.d. = below detection limit (0.06μM); – denotes unavailable data or bed sediment sample

Major elements and Sr isotope data for these samples are in Huh (unpublished data), Huh et al. (1998a, b) and Huh and Edmond (1999)

References

APHA (1998) Standard methods for the examination of water and wastewater, 20th edn. American Public Health Association, Washington

Bethke CM (2002) The Geochemist's Workbench 4.0. Urbana, IL

Beyer L, Pingpank K, Wriedt G, Boelter M (2000) Soil formation in coastal continental Antarctica (Wilkes Land). Geoderma 95(3–4):283–304

Boggs S (2001) Principles of sedimentology and stratigraphy, 3rd edn. Prentice-Hall, Upper Saddle River

Caraco NF (1995) Influence of human population on P transfers to aquatic systems: a regional scale study using large rivers. In: Tiessen H (ed) SCOPE 54—Phosphorus in the global environment. John Wiley & Sons Ltd

Cauwet G, Sidorov I (1996) The biogeochemistry of Lena River: organic carbon and nutrients distribution. Mar Chem 53(3–4):211–227

Collins R, Jenkins A (1996) The impact of agricultural land use on stream chemistry in the Middle Hills of the Himalayas. Nepal J Hydrol 185(1–4):71–86

Colman AS, Mackenzie FT, Holland HD, Van Cappellen P, Ingall ED (1997) Redox stabilization of the atmosphere and oceans and marine productivity, discussion and reply. Science 275(5298):406–408

Compton J, Mallinson D, Glenn CR, Filippelli G, Föllmi K, Shields G, Zanin Y (2000) Variations in the global phosphorus cycle. In: Glenn CR, Prévôt-Lucas L, Lucas J (eds) Marine Authigenesis: From Global to Microbial. SEPM Special Publication, Tulsa, pp 21–33

Cook PJ (1984) Spatial and temporal controls on the formation of phosphate deposits—a review. In: Nriagu JO, Moore PB (eds) Phosphate minerals. Springer-Verlag, Heidelberg, pp 242–274

Cotner JB, Wetzel RG (1992) Uptake of dissolved inorganic and organic phosphorus compounds by phytoplankton and bacterioplankton. Limnol Oceanogr 37(2):232–243

Cross AF, Schlesinger WH (1995) A literature review and evaluation of the Hedley fractionation: applications to the biogeochemical cycle of soil phosphorus in natural ecosystems. Geoderma 64(3–4):197–214

Delaney ML (1998) Phosphorus accumulation in marine sediments and the oceanic phosphorus cycle. Global Biogeochem Cycles 12(4):563–572

Dobson JE, Bright EA, Coleman PR, Durfee RC, Worley BA (2000) LandScan: a global population database for esti-

mating populations at risk. Photogram Eng Remote Sens 66(7):849–857
Dudzinski ML, Norris JM, Chmura JT, Edwards CBH (1975) Repeatability of principal components in samples: normal and non-normal data sets compared. Multivar. Behav Res 10(1):109
Dürr HH, Meybeck M, Dürr SH (2005) Lithologic composition of the Earth's continental surfaces derived from a new digital map emphasizing riverine material transfer. Global Biogeochem. Cycles 19: doi:10.1029/2005GB002515
Edmond JM, Spivack A, Grant BC, Hu M-H, Chen Z, Chen S, Zeng X (1985) Chemical dynamics of the Changjiang Estuary. Cont Shelf Res 4(1–2):17–36
Ekholm P (1994) Bioavailability of phosphorus in agriculturally loaded rivers in southern Finland. Hydrobiologia 287(2):179–194
Fekete B, Vörömarty CJ, Grabs W (2002) High-resolution fields of global runoff combining observed river discharge and simulated water balances. Global Biogeochem. Cycles 16(3): doi:10.1029/1999GB001254
Field AP (2000) Discovering statistics using SPSS for Windows: advanced techniques for the beginners. Sage, London
Filippelli GM, Delaney ML (1994) The oceanic phosphorus cycle and continental weathering during the Neogene. Paleoceanography 9(5):643–652
Filippelli GM (1997) Controls on phosphorus concentration and accumulation in oceanic sediments. Mar Geol 139(1–4):231–240
Fox LE (1989) A model for inorganic control of phosphate concentrations in river waters. Geochim Cosmochim Acta 53(2):417–428
Fox LE (1993) The chemistry of aquatic phosphate: inorganic processes in rivers. Hydrobiologia 253(1–3):1–16
Froelich PN, Bender ML, Luedtke NA, Heath GR, DeVries T (1982) The marine phosphorus cycle. Am J Sci 282(4):474–511
Gaillardet J, Dupré B, Louvat P, Allègre CJ (1999) Global silicate weathering and CO_2 consumption rates deduced from the chemistry of large rivers. Chem Geol 159(1–4):3–30
Global Environmental Monitoring System (1994–1996) Ontario, Canada, United Nations Environment Programme, Global Environmental Monitoring System, Freshwater Quality Program, Collaborating Centre for Freshwater Quality Monitoring and Assessment at the National Water Research Institute of Environment Canada, Burlington. http://www.gemswater.org/publications/index-e.htm. Cited 24 Feb, 2006
Guidry MW, Mackenzie FT (2000) Apatite weathering and the Phanerozoic phosphorus cycle. Geology 28(7):631–634
Guidry MW, Mackenzie FT, Arvidson RS (2000) Role of tectonics in phosphorus distribution and cycling. In: Glenn CR, Prévôt-Lucas L, Lucas J (eds) Marine authigenesis: from global to microbial. SEPM Special Publication, Tulsa, pp 35–51
Guidry MW, Mackenzie FT (2003) Experimental study of igneous and sedimentary apatite dissolution: control of pH, distance from equilibrium, and temperature on dissolution rates. Geochim Cosmochim Acta 67(16):2949–2963
Guo L, Zhang J-Z, Gueguen C (2004) Speciation and fluxes of nutrients (N, P, Si) from the upper Yukon River. Global Biogeochem. Cycles 18: doi:10.1029/2003GB002152
Harrison JA, Seitzinger SP, Bouwman AF, Caraco NF, Beusen AHW, Vörösmarty CJ (2005) Dissolved inorganic phosphorus export to the coastal zone: results from a spatially explicit, global model. Global Biogeochem. Cycles 19: doi:10.1029/2004GB002357
Hearn PP Jr, Hare TM, Schruben P, Sherrill D, LaMar C, Tsushima P (2000) Global GIS Database: Digital Atlas of South Asia. U.S. Geological Survey
Hearn PP Jr, Hare TM, Schruben P, Sherrill D, LaMar C, Tsushima P (2001) Global GIS: North Eurasia. U.S. Geological Survey & American Geological Institute
Hearn PP Jr, Hare TM, Schruben P, Sherrill D, LaMar C, Tsushima P (2003) USGS Global GIS (Version 6.2). The American Geological Institute
Holmes RM, Peterson BJ, Gordeev VV, Zhulidov AV, Meybeck M, Lammers RB, Vörösmarty CJ (2000) Flux of nutrients from Russian rivers to the Arctic Ocean: can we establish a baseline against which to judge future changes? Water Resour Res 36(8):2309–2320
Holmes RM, Peterson BJ, Zhulidov AV, Gordeev VV, Makkaveev PN, Stunzhas PA, Kosmenko LS, Kohler GH, Shiklomanov AI (2001) Nutrient chemistry of the Ob' and Yenisey Rivers, Siberia: results from June 2000 expedition and evaluation of long-term data sets. Mar Chem 75(3):219–227
House WA, Denison FH, Armitage PD (1995) Comparison of the uptake of inorganic phosphorus to a suspended and stream bed-sediment. Water Res 29(3):767–779
House WA, Denison FH (1998) Phosphorus dynamics in a lowland river. Water Res 32(6):1819–1830
House WA (2003) Geochemical cycling of phosphorus in rivers. Appl Geochem 18(5):739–748
Huh Y, Tsoi M-Y, Zaitsev A, Edmond JM (1998a) The fluvial geochemistry of the rivers of Eastern Siberia: I. Tributaries of the Lena River draining the sedimentary platform of the Siberian Craton. Geochim Cosmochim Acta 62(10):1657–1676
Huh Y, Panteleyev G, Babich D, Zaitsev A, Edmond JM (1998b) The fluvial geochemistry of the rivers of Eastern Siberia: II. Tributaries of the Lena, Omoloy, Yana, Indigirka, Kolyma, and Anadyr draining the collisional/accretionary zone of the Verkhoyansk and Cherskiy ranges. Geochim Cosmochim Acta 62(12):2053–2075
Huh Y, Edmond JM (1999) The fluvial geochemistry of the rivers of eastern Siberia; III, Tributaries of the Lena and Anabar draining the basement terrain of the Siberian Craton and the Trans-Baikal Highlands. Geochim Cosmochim Acta 63(7–8):967–987
Hutcheson G, Sofroniou N (1999) The multivariate social scientist. SAGE, London
Ilyin AV, Krasilnikova NA (1989) Igneous Proterozoic-Cambrian phosphate resources in eastern Siberia, USSR. In: Notholt AJG, Sheldon RP, Davidson DF (eds) Phosphate deposits of the world, vol. 2, Phosphate rock resources. Cambridge Univ Press, Cambridge, U.K., pp 510–513
Kaiser HF, Rice J (1974) Little Jiffy, Mark IV. Educ Psychol Meas 34:111–117
Koerselman W, Vankerkhoven MB, Verhoeven JTA (1993) Release of inorganic N, P and K in peat soils; effect of temperature, water chemistry and water-level. Biogeochemistry 20(2):63–81

Lara RJ, Rachold V, Kattner G, Hubberten HW, Guggenberger G, Skoog A, Thomas DN (1998) Dissolved organic matter and nutrients in the Lena River, Siberian Arctic: characteristics and distribution. Mar Chem 59(3–4):301–309

Li Y (1986) Regional review; China. In: Cook PJ, Shergold JH (eds) Proterozoic and cambrian phosphorites. Cambridge University Press, Cambridge, UK

Li Y-H (2000) A compendium of geochemistry, from solar nebula to the human brain. Princeton University Press, Princeton, NJ

Liu SM, Zhang J, Chen HT, Wu Y, Xiong H, Zhang ZF (2003) Nutrients in the Changjiang and its tributaries. Biogeochemistry 62(1):1–18

Meybeck M (1982) Carbon, nitrogen, and phosphorus transport by world rivers. Am J Sci 282(4):401–450

Meybeck M (1993) Riverine transport of atmospheric carbon: sources, global typology and budget. Water Air Soil Pollut 70(1–4):443–463

Meybeck M, Ragu A (1996) River discharges to the oceans: an assessment of suspended solids, major ions and nutrients. UNEP Publication, Nairobi, Kenya

Moon S, Huh Y, Qin J, Nguyen vP (2007) Chemical weathering in the Hong (Red) River basin: rates of silicate weathering and their controlling factors. Geochim Cosmochim Acta 71:1411–1430

Nash WP (1984) Phosphate minerals in terrestrial igneous and metamorphic rocks. In: Nriagu JO, Moore PB (eds) Phosphate minerals. Springer-Verlag, Heidelberg, pp 215–241

Notholt AJG (1980) Igneous apatite deposits; mode of occurrence, economic development and world resources. In: Sheldon RP, Burnett WC (eds) Fertilizer mineral potential in Asia and the Pacific. East-West Resour Syst Inst, Honolulu, pp 263–286

Notholt AJG, Sheldon RP, Cook PJ, Shergold JH (1986) Regional review; world resources. In: Cook PJ, Shergold JH (eds) Proterozoic and cambrian phosphorites. Cambridge University Press, Cambridge, UK, pp 10–19

Okin GS, Mahowald N, Chadwick OA, Artaxo P (2004) Impact of desert dust on the biogeochemistry of phosphorus in terrestrial ecosystems. Global Biogeochem Cycles 18: doi:10.1029/2003GB002145

Qin J, Huh Y, Edmond JM, Du G, Ran J (2006) Chemical and physical weathering in the Min Jiang, a headwater tributary of the Yangtze River. Chem Geol 227:53–69

Rudnick RL, Gao S (2004) Composition of the Continental Crust. In: Rudnick RL (ed) Treatise on geochemistry, vol 3. Elsevier, pp 1–64

Ruttenberg KC, Berner RA (1993) Authigenic apatite formation and burial in sediments from non-upwelling, continental margin environments. Geochim Cosmochim Acta 57(5):991–1007

Ruttenberg KC (2004) The global phosphorus cycle. In: Schlesinger WH (ed) Treatise on geochemistry, vol. 8. Elsevier, pp 585–643

Schenau SJ, Reichart GJ, De Lange GJ (2005) Phosphorus burial as a function of paleoproductivity and redox conditions in Arabian Sea sediments. Geochim Cosmochim Acta 69(4):919–931

Seitzinger SP, Hartnett H, Lauck R, Mazurek M, Minegishi T, Spyres G, Styles R (2005) Molecular-level chemical characterization and bioavailability of dissolved organic matter in stream water using electrospray-ionization mass spectrometry. Limnol Oceanogr 50(1):1–12

Sferratore A, Billen G, Garnier J, Théry S (2005) Modeling nutrient (N, P, Si) budget in the Seine watershed: application of the Riverstrahler model using data from local to global scale resolution. Global Biogeochem Cycles 9: doi:10.1029/2005GB002496

Shan Y, McKelvie ID, Hart BT (1994) Determination of alkaline phosphatase-hydrolyzable phosphorus in natural water systems by enzymatic flow injection. Limnol Oceanogr 39(8):1993–2000

Smith SV, Swaney DP, Talaue-McManus L, Bartley JD, Sandhei PT, McLaughlin CJ, Dupra VC, Crossland CJ, Buddemeier RW, Maxwell BA, Wulff F (2003) Humans, hydrology, and the distribution of inorganic nutrient loading to the ocean. Bioscience 53(3):235–245

Summerfield MA, Hulton NJ (1994) Natural controls of fluvial denudation rates in major world drainage basins. J Geophys Res 99(7):13871–13883

Taylor AW, Kunish HM (1971) Phosphate equilibria on stream sediment and soil in a watershed draining an agricultural region. J Agric Food Chem 19(5):827–831

Tran QA, Nguyen DK (1986) Deposits; Lao Cai, Vietnam. In: Cook PJ, Shergold JH (eds) Proterozoic and cambrian phosphorites. Cambridge Univ. Press, Cambridge, UK, pp 155–161

Turner RE, Rabalais NN, Justić D, Dortch Q (2003) Global patterns of dissolved N, P and Si in large rivers. Biogeochemistry 64(3):297–317

Wang B, Clemens SC, Liu P (2003) Contrasting the Indian and East Asian monsoons; implications on geologic timescales. Mar Geol 201(1–3):5–21

White AF, Blum AE (1995) Effects of climate on chemical weathering in watersheds. Geochim Cosmochim Acta 59(9):1729–1747

Wu L, Huh Y, Qin J, Du G, van Der Lee S (2005) Chemical weathering in the Upper Huang He (Yellow River) draining the eastern Qinghai-Tibet Plateau. Geochim Cosmochim Acta 69(22):5279–5294

Yan W, Zhang S (2003) The composition and bioavailability of phosphorus transport through the Changjiang (Yangtze) River during the 1998 flood. Biogeochemistry 65:179–194

Zakharova EA, Pokrovsky OS, Dupré B, Zaslavskaya MB (2005) Chemical weathering of silicate rocks in Aldan Shield and Baikal Uplift; insights from long-term seasonal measurements of solute fluxes in rivers. Chem Geol 214(3–4):223–248

Zhang J (1996) Nutrient elements in large Chinese estuaries. Cont Shelf Res 16(8):1023–1045

Zhang C, Tian H, Liu J, Wang S, Liu M, Pan S, Shi X (2005) Pools and distributions of soil phosphorus in China. Global Biogeochem. Cycles 19: doi:10.1029/2004GB002296